Cretaceous Research 114 (2020) 104525

Contents lists available at ScienceDirect

Cretaceous Research

journal homepage: www.elsevier.com/locate/CretRes

Fungus–plant interactions in Aptian Tropical Equatorial Hot arid belt: White rot in araucarian wood from the Crato fossil Lagerstätte (Araripe Basin, Brazil)

Ângela Cristine Scaramuzza dos Santos [a], Margot Guerra-Sommer [a,*], Isabela Degani-Schmidt [b], Anelise Marta Siegloch [a], Ismar de Souza Carvalho [c], João Graciano Mendonça Filho [d], Joalice de Oliveira Mendonça [d]

[a] Universidade Federal do Rio Grande do Sul, IGEO, Programa de Pós-Graduação em Geociências, Av. Bento Gonçalves 9500, Porto Alegre, 91509-900, Brazil
[b] Universidade Federal do Rio de Janeiro, CCMN/IGEO, Programa de Pós-Graduação em Geologia, Av. Athos da Silveira Ramos, 274, Bloco J1, Cidade Universitária, Rio de Janeiro, RJ, 21941-916, Brazil
[c] Universidade Federal do Rio de Janeiro, CCMN/IGEO, Departamento de Geologia, Av. Athos da Silveira Ramos, 274, Bloco J1, Cidade Universitária, Rio de Janeiro, RJ, 21941-916, Brazil
[d] Universidade Federal do Rio de Janeiro, CCMN/IGEO, Departamento de Geologia, LAFO-Laboratório de Palinofáceis e Fáceis Orgânica, Av. Athos da Silveira Ramos, 274, Bloco J1, Sala 20, Rio de Janeiro, RJ, 21941-916, Brazil

A R T I C L E I N F O

Article history:
Received 17 July 2019
Received in revised form 19 May 2020
Accepted in revised form 21 May 2020
Available online 30 May 2020

Keywords:
Basidiomycetes
Gymnosperms
Wood anatomy
Fungal decay
Fungus-plant interactions

A B S T R A C T

For the first time, this study describes the dynamics of white rot fungal decay in a petrified conifer branch with clear araucarian affinity from the late Aptian Crato Lagerstätte (Santana Formation, Araripe Basin, northeastern Brazil). High resolution optical microscopy was used to identify tridimensional chemical and anatomical evidence in different regions of the bark and xylem tissues of permineralized shoots, and results support the hypothesis that the host responded to disease that may have started when it was still alive. The wood decay pattern was strongly indicative of the selective decay by white rot. The general pattern of interaction is consistent with pathogenic rather than saprophytic fungal activity. Analysis of fungus–plant interactions associated with growth ring patterns imply intermittent periods of favorable temperature-moisture inputs that were crucial for fungal activity during the deposition of the Crato fossil Lagerstätte included in the Tropical Equatorial Hot arid belt.

1. Introduction

It is currently known that the macroflora of the late Aptian Lagerstätte of the Crato Member (Araripe Basin, northeastern Brazil) consisted of angiosperms (32%), conifers (30%), gnetaleans (19%), and lycophytes, sphenophytes, filicophytes, pteridosperms, bennettitaleans, and gymnosperms *incertae sedis* (19%) (Table 1, updated from Bernardes-de-Oliveira et al., 2014). The conifers described to date from laminated carbonates deposited in the Crato paleolake that lay within the Tropical Equatorial Hot arid belt (Chumakov et al., 1995) belonged to the families Cheirolepidiaceae and Araucariaceae. Many plant taxa from the Crato Lagerstätte adapted to the dry paleoenvironmental conditions and unfavorably dry climate in the Tropical Equatorial Hot arid belt, as evidenced by sunken stomata, increased cuticle and epidermis thicknesses, and the development of papillae and hairs (Dilcher et al., 2005; Feild et al., 2004; Mohr et al., 2006, 2007).

The main goal of the present study is to fill gaps in the knowledge of plant–fungus interaction in the late Aptian Tropical Equatorial Hot arid belt. The working hypothesis of the present study is based on a sample of petrified conifer wood that shows evidence of fungal decay. Although it is assumed that the wood was derived from a hot arid environment, the paleoclimatic context of the white rot decay record from the Late Devonian to the Eocene (Table 2) comprised at least sporadic phases of humidity. Anatomical analysis of the well-preserved specimen that was complete with pith, secondary xylem, and bark, enabled taxonomic identification and observations of the three-dimensional development of degradation patterns and chemical and anatomical responses of the host wood to the disease. This provides advantages over previous studies

* Corresponding author.
E-mail address: margot.sommer@ufrgs.br (M. Guerra-Sommer).

https://doi.org/10.1016/j.cretres.2020.104525

Table 1
Macrofloral biodiversity of the Crato Lagerstätte (updated from Bernardes-de-Oliveira et al., 2014).

Name	References
Lycophytes	
Isoetes	Bernardes-de-Oliveira et al. (2003)
Sphenophytes	
Schizoneura	Dilcher et al. (2000)
Filicophytes	
Ruffordia goeppertii	Mohr et al. (2015)
Pteridospermales	
Caytoniales	Fanton et al. (2007a, b)
Bennettiales	
Ptilophyllum	Duarte (1985)
Coniferales	
Duartenia araripensis	Mohr et al. (2012)
Pseudofrenelopsis capillata	Sucerquia et al. (2015)
Tomaxellia biforme	Kunzmann et al. (2006)
Araucaria sp.	Kunzmann et al. (2004)
Araucarites/Araucaria cartellei e *A. imponens* (Sec. Columbea)	Duarte (1993); Sucerquia (2006)
Araucariostrobus sp.	Kunzmann et al. (2004)
Brachyphyllum obesum	Duarte (1985); Kunzmann et al. (2004); Batista et al. (2017)
Lindleycladus sp.	Kunzmann et al. (2004)
Gnetales	
Cratonia cotyledon	Rydin et al. (2003)
Priscowelwitschia austroamericana	Dilcher et al. (2005)
Welwitschiophyllum brasiliense	Dilcher et al. (2005)
Welwitschiostrobus murili	Dilcher et al. (2005)
Ephedra paleoamericana	Kerkhoff and Dutra (2007)
Cearania heterophylla	Kunzmann et al. (2009)
Cariria orbiculiconiformes	Kunzmann et al. (2011)
Itajuba yansanae	Ricardi-Branco et al. (2013)
Friedsellowia gracilifolia	Löwe et al. (2013)
Incertae sedis gymnosperms	
Novaolinda dubia	Kunzmann et al. (2007)
Angiosperms	
Jaguariba wiersemana	Coiffard et al. (2013)
Pluricarpellatia peltata	Mohr et al. (2008)
Klitzschophyllites flabellatus	Mohr and Rydin (2002); Mohr et al. (2006)
Endressinia brasiliana	Mohr and Bernardes-de-Oliveira (2004)
Schenkeriphyllum glanduliferum	Mohr et al. (2013)
Araripia florifera	Mohr and Eklund (2003)
Iara iguassu	Fanton et al. (2007a, b)
Hexagyne philippiana	Coiffard et al. (2014)
Cratolirion bognerianum	Coiffard et al. (2019)
Cratosmilax jacksoni	Lima et al. (2014)
Spixiarum kipea	Coiffard et al. (2014)

based on gymnosperms woods, where it was not possible to determine the original extent of the fungal infection, mainly due to the incompleteness of the specimens due to fossil fragmentation from taphonomic processes (Falcon-Lang et al., 2001; Pujana et al., 2009; García-Massini et al., 2012; Gnaedinger et al., 2015; Wan et al., 2016; Sagasti et al., 2019).

2. Geological synthesis

The Araripe Basin (Fig. 1) is a hinterland basin covering an area of 12,200 km^2 that originated during a Berriasian-Hauterivian tectonic phase connected with the first stages of South America and Africa rifting (Matos, 1992; Carvalho, 2000). Situated above a major unconformity representing a significant hiatus, the post-rift stage of the Araripe Basin is represented by deposits of the Araripe Group that cover the late Aptian to the early Albian (Coimbra et al., 2003). According to Assine (2007), low subsidence during this stage resulted in the deposition of deltaic to lacustrine sediments (Rio das Batateiras Formation and Crato Member, Santana Formation), followed by evaporites (Ipubi Member, Santana Formation) and marginal marine shales (Romualdo Member of Santana Formation and Arajara Formation).

Based on the widespread occurrence of evaporites along the evolving South Atlantic rift system, the absence of coal deposits, and the dominance of drought-resistant, xerophytic vegetation (Ziegler et al., 2003; Mohr et al., 2007), it is assumed that semi-arid to arid climatic conditions predominated during the deposition of the Araripe Basin, which was situated within the Tropical Equatorial Hot arid belt of Chumakov et al. (1995) in late Early Cretaceous times. Scherer et al. (2015) integrated sedimentological and paleoclimatic data in the Aptian succession of the Araripe Basin that point to the existence of consistently high temperatures, albeit with variable humidity. Sedimentological evidence indicates that, despite variations in the oxygenation degrees of the lakes, the climate was relatively humid or sub humid, and that no major climatic changes occurred during the deposition of the basal sequences. Furthermore, Goldberg et al. (2019) determined that the strong marine influence was already established during the deposition of the Ipubi layers (sensu Assine, 2007).

The Santana Formation (sensu Ponte and Appi, 1990) is a 60 m thick succession of fine laminated carbonates interlayered with green shales and fine-to-coarse sandstones. The lowermost Crato Member, which is the focus of this study, hosts the Crato fossil Lagerstätte. Soft tissues, color patterns, and fine details of plants,

Table 2
Indirect and direct records of white rot decay in woods from the Devonian to the Eocene.

Interval	Evidence		Climatic zones (Scotese, 2011, 2014)	References
	Direct	Indirect		
Late Devonian	x	x	Warm/arid	Stubblefield et al. (1985)
Mississipian	x		Tropical	Krings et al. (2011)
Middle Pensilvanian	x		Tropical	Dennis (1969, 1970)
Early Permian	x	x	Tropical	Wan et al. (2017)
	x	x	Tropical	Barthel (2010)
Middle − late Permian	x		Cool Temperate	Wei et al. (2016)
Late Permian	x	x	Cool Temperate	Stubblefield and Taylor (1986)
		x	Warm	Diéguez and López-Gomez (2005)
	x	x	Cool Temperate	Wan et al. (2016)
		x	Cool Temperate	Wei et al. (2019)
	x	x	Cold	Weaver et al. (1997)
Early Triassic		x	Warm	Stubblefield and Taylor (1986)
Late Triassic		x	Tropical	Creber and Ash (1990)
Early Jurassic	x	x	Warm Temperate	Gnaedinger et al. (2015)
Middle Jurassic	x	x	Warm	Feng et al. (2015)
	x	x	Warm	García-Massini et al. (2012)
Middle/Late Jurassic			Warm	Sagasti et al. (2019)
Early Cretaceous	x	x	Boreal Tropical	Tian et al. (2020)
Mid-Cretaceous		x	Cool	Falcon Lang et al. (2001)
Late Eocene		x	Warm	Pujana et al. (2009)
Early Cretaceous		x	Arid	This paper

invertebrates, and vertebrates are preserved within the carbonatic succession (Carvalho et al., 2019; Grimaldi, 1990; Martill and Bechly, 2007; Naish, 2007; Pinheiro et al., 2012), and a late Aptian age (119−113 Ma) can be inferred for this interval from palynological data (Rios-Netto et al., 2012).

Heimhofer and Hochuli (2010) inferred that the bulk of limestone from the Crato Member was formed via the authigenic precipitation of calcite. Microfacies analysis (Catto et al., 2016) indicated that the limestones were genetically associated with lacustrine systems in a negative hydric balance. Neumann et al. (2003) and Martill and Bechly (2007) considered that hypersaline lakes with low oxygen concentrations would have developed under low energy and shallow waters that are associated with high evaporation. However, the influence of marine waters (with strongly fluctuating salinities) has clearly been demonstrated for other stratigraphic units of the basin.

3. Material and methods

The specimen analyzed in this study is a petrified wood that is likely a secondary branch (length 395 mm; mean diameter 21 mm). While removing it from the carbonate sediment, it broke into seven fragments. In general, the solidity of the wood is intact, preservation is generally good, and the anatomical features are clearly observable. The specimen is housed in the paleontological collection of the Departamento de Geologia, Instituto de Geociências, Universidade Federal do Rio de Janeiro under the acronym 2443Pb, and thin sections are stored under the codes 2443Pb-1 to 35.

3.1. Fossil preparation and observation

Successive transverse (7 slides), radial (14 slides), and tangential sections (14 slides) were made from seven different fragments of the single branch to observe the anatomical structure and three-dimensional development of degradation. Successive descriptions of the fungus decay spectrum were made along the entire wood sample from the periphery of the bark to the outer, central, and innermost secondary xylem of the sample (Fig. 2). Since the branch was narrow, every single slide comprised all tissues from border to border. The methodology adopted was similar to that used by Harper et al. (2018) for a pteridophyte stem but considering the peculiarities of fungal pathogenic attack in a gymnospermous wood.

Polished and uncoated thin sections (40 μm thick) were produced from material that was highly mineralized by iron minerals, which frequently impaired observations of anatomical details. Epoxy resin was used as an embedding and mounting medium. The sections were polished using 0.05 mm aluminum oxide powder.

An anatomical analysis was conducted under transmitted and reflected light microscopy. However, attempts were made to observe the anatomy of the wood under scanning electron microscopy (SEM) following standard techniques, but these were unsuccessful.

The thin sections were examined and pictures were taken with a Leica S8 APO stereoscopic microscope with a mounted camera, a Zeiss AxioScope A1 transmitted light microscope with an AxioCam MRc camera (located at UFRGS), and a Zeiss AxioScope 2 Plus reflected light microscope equipped with a spectrophotometer J&M (MSP 200) through a 50× objective lens (located at UFRJ).

The images were analyzed, and measurements were taken using Zeiss Axio Vision 4.8.1 software. Plates were composed using Adobe Photoshop CS3 Extended. Transformations were made to the images using cropping, rotation, contrast adjustments, focus stacking, and image composition. The terminology used to provide anatomical details of the wood followed the recommendations of Richter et al. (2004).

The elemental composition of cell walls and infillings of cell lumina were analyzed using an energy dispersive spectroscopy (EDS) detector coupled to an Inspect F50 FEI SEM located at the Centro de Microscopia e Microanálises IDEIA at Pontifícia Universidade Católica do Rio Grande do Sul, and employing the same slides as those used to conduct anatomical analyses (which had been gold-coated to conduct the unsuccessful SEM observations).

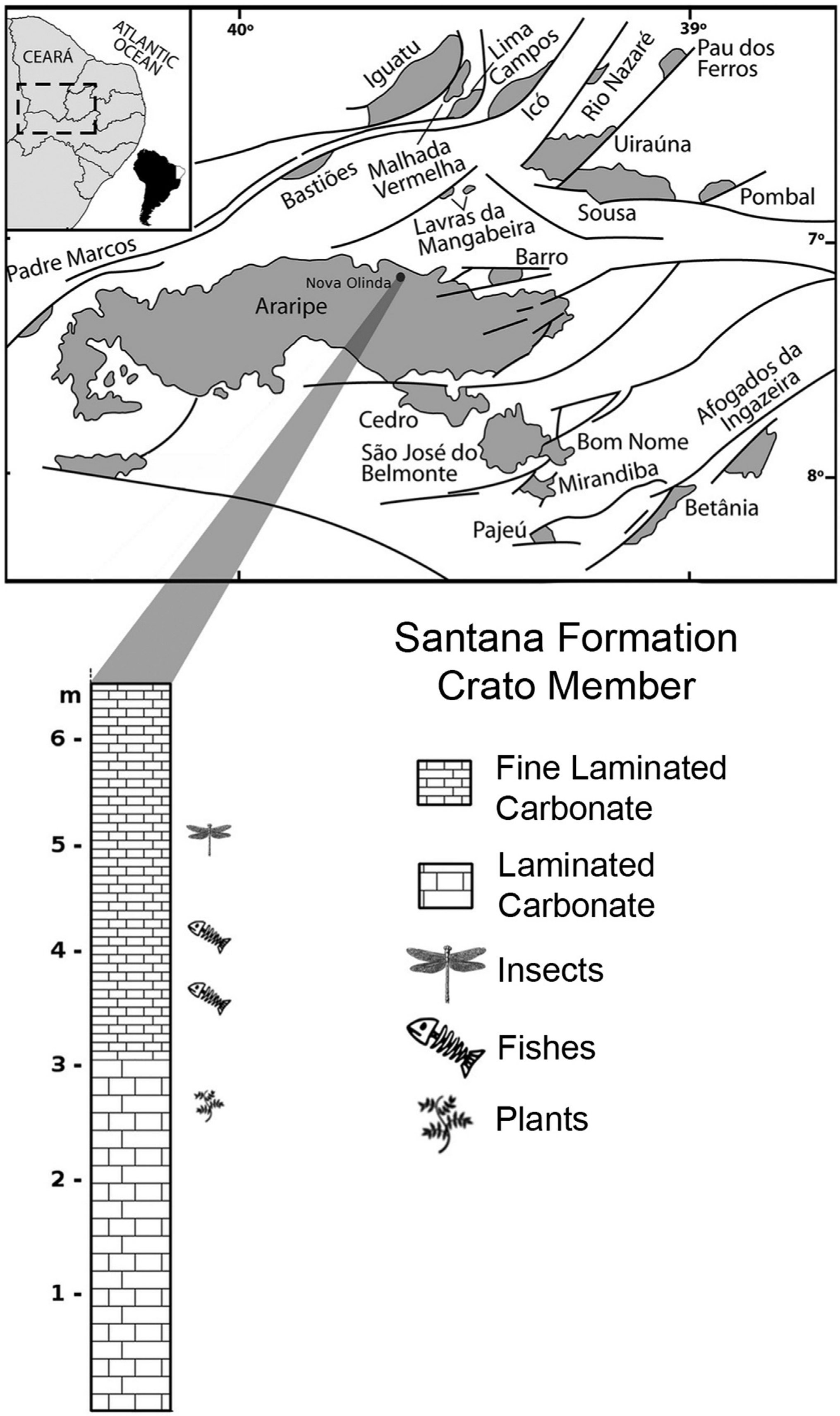

Fig. 1. Location map of the Araripe Basin in the context of the Cretaceous Brazilian Northeastern intracratonic basins and stratigraphic profile of the collection site Pedra Branca Mine, Nova Olinda County, Brazil (Carvalho et al., 2019).

4. Results and discussion

4.1. Wood petrification process

Elemental EDS analysis indicates that the wood petrifaction process involved partial degradation of organic components and mineralization by dominant iron minerals (Fe), oxygen (O), besides carbon (C) in the cell walls and in massive dark areas of the sample, whereas the mineralization of anatomical voids corresponding to cell lumina mainly occurred with respect to crystal-shaped calcium (Ca) (Fig. 3). Therefore, wood fossilization resulted from a combination of permineralization and replacement processes.

4.2. Main anatomical wood patterns: systematic, climatic, and ecological constraints

The specimen is a piece of gymnospermous wood (ca. 21 mm in diameter) composed of a very small pith with irregular boundaries surrounded by a massive homogeneous secondary xylem (up to 16 mm wide). The wood tissue is surrounded by poorly preserved bark (2 mm wide). Given the diagnostic features (the presence of compression wood, leaf traces, and a leaf organically connected to the axis), the specimen is determined to be a branch (Fig. 4).

The small, heterogeneous pith (ca. 0.5 mm in diameter) is composed of rounded or polygonal parenchymatous cells in cross-section and dispersed sclerenchymatous clusters. The thick zone of the secondary xylem shows a typical gymnospermous pycnoxylic pattern and is composed of elongated tracheids and transverse parenchyma rays. In cross-section, the tracheid outline is square to polygonal and ca. 70 μm in diameter (9 μm mean wall thickness). The tracheids are arranged in regular rows and are limited by elongated, rectangular, parenchymatous ray cells with thin walls (3 μm) that show a uniseriate disposition.

Four to five growth rings with variable widths (680–948 μm) are observed in the transversal mesoscopic view of the seven fragments from the single specimen. These are seen to be uneven under higher magnification, and they are characterized by a very low proportion of latewood composed of only one or two tracheids with reduced radial diameters and no significant increases in wall thickness. These factors associated with high ring width variability imply stressful growing conditions (Fig. 4A, B). In addition, the subtle discontinuous ring boundaries of some of the growth rings (Fig. 4B) indicate that they were formed during a short-term reduction in cambial activity.

In longitudinal radial sections (Fig. 5), the tracheids mainly show crowded triseriate (rarely biseriate), alternate, areolated pitting with flattened borders and hexagonal boundaries, in addition to rounded or slightly elliptical apertures (Fig 5A). The pit spacing on the tracheid radial walls has a compact arrangement from margin to margin; this is a striking anatomical feature that is present from the initial to the outer rows of the secondary xylem, in both the early and late wood (Fig. 5B). Crossfields are wide, showing typical elongated parenchyma cells with thin walls; in some areas it is possible to observe that crossfield pits are crowded and have an araucarioid pattern, which according to the criteria of IAWA (Richter et al., 2004) consists of numerous, densely arranged pits with cupressoid organization (Fig. 5C, D).

The presence of resin plugs in the tracheids (Fig. 6A) has a diagnostic value for the extant genera *Agathis* and *Araucaria* (Richter et al., 2004). Axial parenchyma was not observed in either radial or tangential sections.

Longitudinal tangential sections showed the presence of uniseriate rays that are between one and fourteen cells high (six cells on average), at a density of six rays per millimeter (Fig. 6B). The tangential surfaces of the ray cells are not pitted.

The xylem is encircled by a poorly preserved vascular cambium comprising one to two subrectangular cells. The non-collapsed, conducting secondary phloem region (0.95 mm mean thickness) is also poorly preserved, but frequent irregularly shaped lacunae are evident (Fig. 7A). In the region of the collapsed secondary phloem, there was a belt of stone cells and canals (Fig. 7A, B). Tangential lacunae occur in areas originally occupied by the rhytidome, and lenticels occur in the outer surface (Fig. 7C).

The constancy of the tracheid pitting characteristics (which occur in a compact arrangement from margin to margin all along the wood), coupled with those of the crossfield pitting showing a constant araucarioid organization, and the presence of resin plugs in the tracheids, exceed the morphotype criteria established by Philippe and Bamford (2008) for characterizing *Agathoxylon* Hartig, and suggest that the specimen has a biological affinity with the extant coniferous family Araucariaceae. In addition to the xylem pattern, the occurrence of canals in the phloem (Kershaw and Wagstaff, 2001) corroborate this affinity. Furthermore, the anatomical features are more consistent with *Araucaria* (sensu Greguss, 1955) than with other genera in the family.

Previously described fossil remains from the Crato Member also support the hypothesis that our specimen has an araucarian affinity. Such fossils are represented by *Araucaria cartellei* leaves (Duarte, 1993), *Araucariostrobus* sp. cones (Kunzmann et al., 2004), and branches of *Brachyphyllum obesum* (Duarte, 1985; Kunzmann et al., 2004; Batista et al., 2017). The macroscopic occurrences are also supported by palynological data (Heimhofer and Hochuli, 2010; Souza-Lima and Silva, 2018).

Wood patterns of Araucariaceae in the Gondwanan Mesozoic were previously recorded for the Jurassic in Chile by Gnaedinger et al. (2015), for the Jurassic in Argentina by García-Massini et al. (2012) and Sagasti et al. (2019), and for the Early Cretaceous in Argentina by Vera and Césari (2012).

In addition, the substantial presence of conifers in the Crato Lagerstätte (Table 2) contradicts the conclusion of Spicer and Skelton (2003) who found no evidence of tropical humidity that was high enough to have supported expressive terrestrial productivity within the Tropical Equatorial Hot arid belt in the early Cretaceous greenhouse climate.

The potential use of araucarians for palaeoenvironmental reconstruction relates to their past and present distributions, and shows that they have a preference for subtropical or mesothermal environments (Kershaw and Wagstaff, 2001). Therefore, available ecological data about Araucariaceae and the growth-ring pattern of the specimen in this study suggest that the plant grew in conditions compatible with the Tropical Equatorial Hot arid belt (Chumakov et al., 1995) with the occurrence of environmental cycles controlled by alternations in water availability (Schweingruber, 1996).

4.3. Fungal remains

Fungal remains are present in the host tissues as scattered fungal bodies and hyphae. Most of them do not possess diagnostic features allowing correlations with extant taxa.

Fungal hyphae (Fig. 8) are present mainly in the xylem tissue and less commonly in the bark. Some propagules are smooth

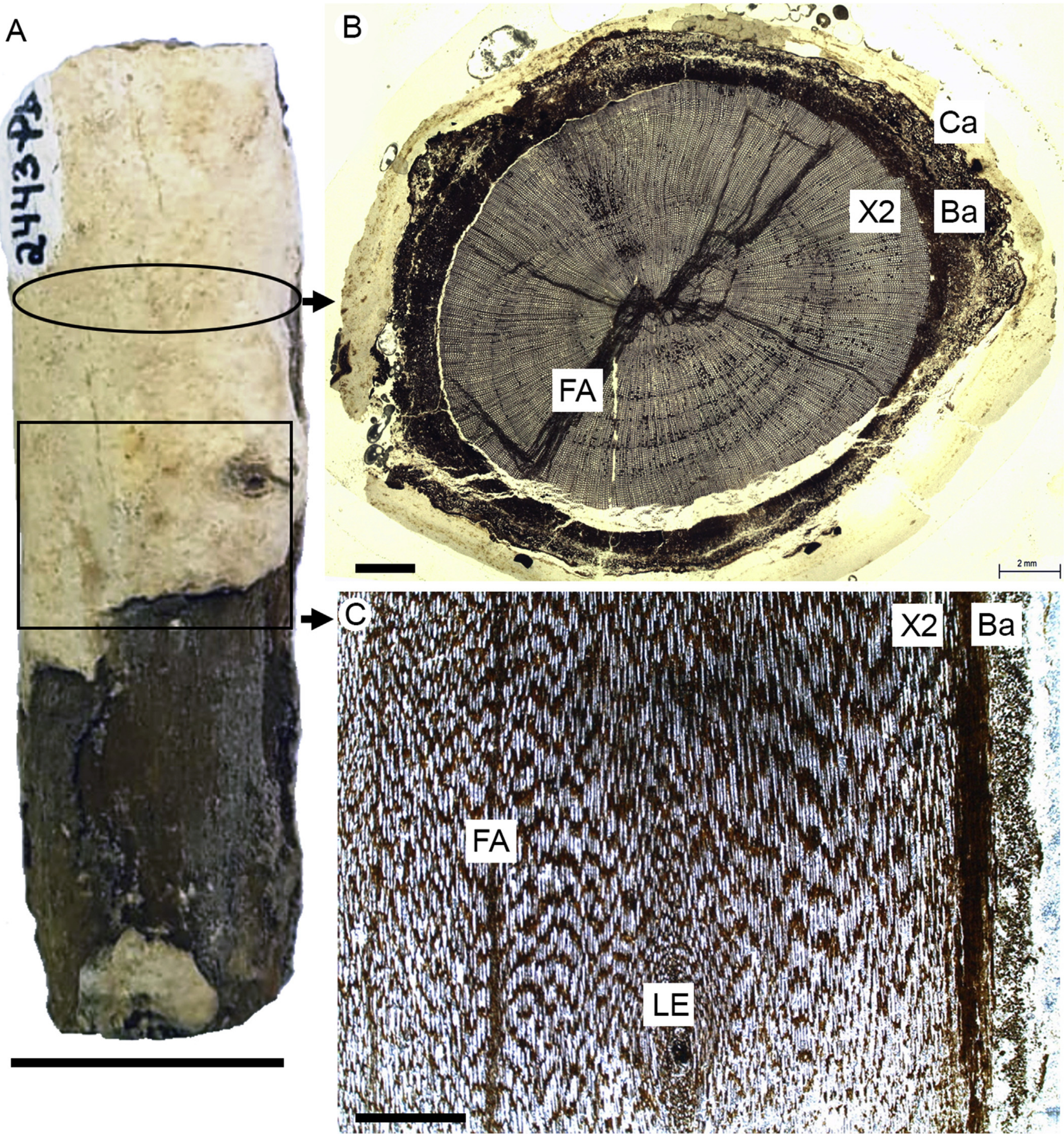

Fig. 2. Schematic illustration of the sections made from the seven branch fragments (specimen 2443-Pb). A) Branch fragment; B) cross section; C) longitudinal section. Ba: bark; Ca: carbonate layer; FA: fungal attack; LE: leaf emergence; X2: secondary xylem. Scale bars: A) 2 cm; B, C) 2 mm. For more details see Material and Methods section.

walled (8 μm average diameter) and tubular shaped, non-septate (Fig. 8A, B) or septate (Fig. 8C) and occur in relatively straight (Fig. 8A, B) or curving course (Fig. 8C). They commonly travel intracellulary, either extending parallel to the long axis of the tracheids (Fig. 8A) or can be traced cross-cutting tracheid lumen (Fig. 8C). Terminal ellipsoidal hypha swellings physically connected to a portion of the intercellular parental hypha commonly found within tracheid lumina (Fig. 8D) and bark cells were identified as conidia of ascomycetes (see Harper et al., 2018).

Unbranched hyphae were found in both xylem and phloem tissues displaying straight tubular shape (15.3 μm average diameter) crossing cells (Fig. 8E) with lateral, randomly arranged emergencies from the main axis (Fig. 8F). Septa are irregularly spaced and connected to the hypha walls at right angles (Fig. 8G).

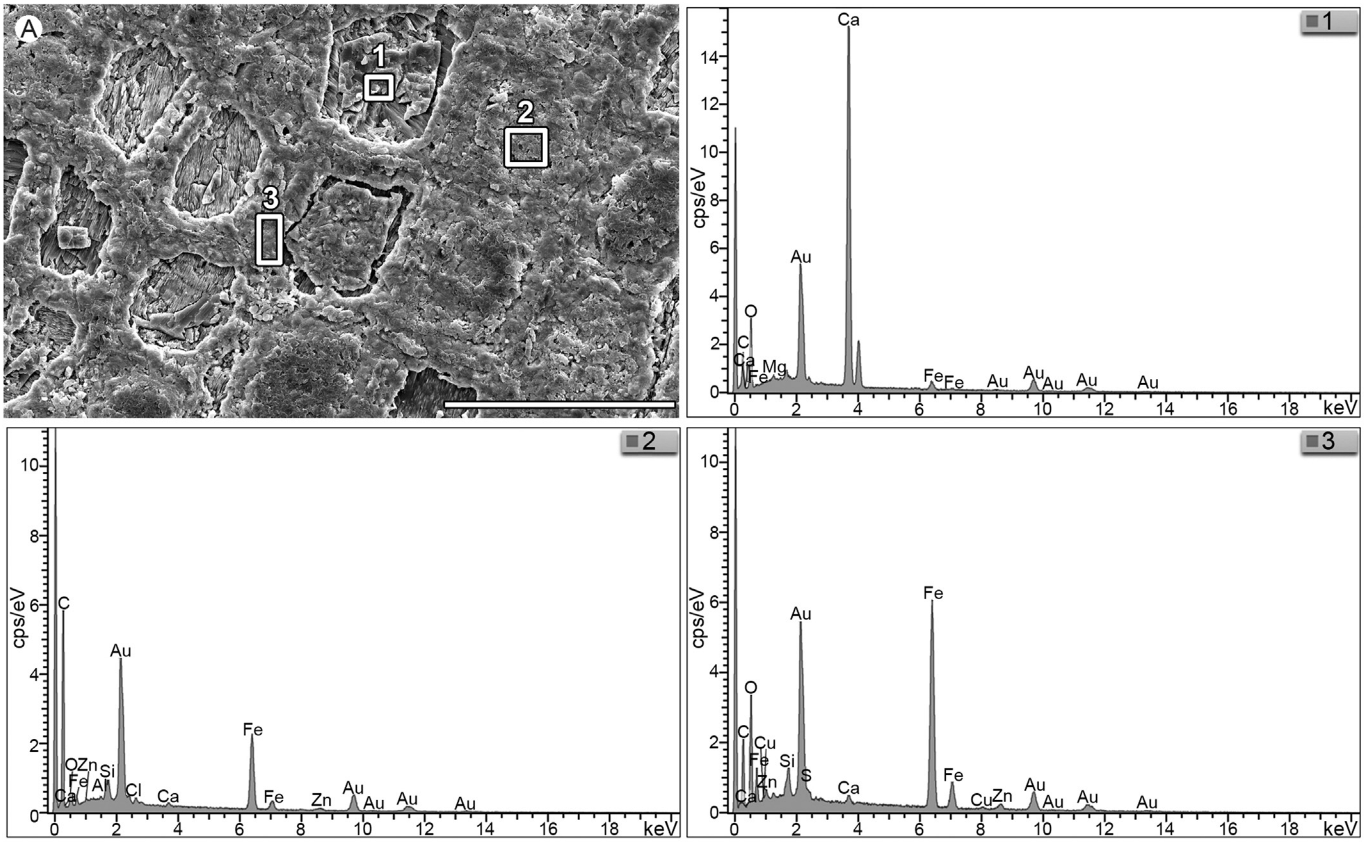

Fig. 3. EDS semi-quantitative results showing chemical composition of cell walls and cell lumen (specimen 2443-Pb). A) Location of performed measurements (1–3). Scale bar: 100 μm.

Some structures found within bark cells and in the lumina of peripheral tracheids were presumed to represent terminal microsclerotia connected to the cell wall by hypha strands (Fig. 9A, B). A probable incomplete, apically branched conidiophore bearing radiating short arms (Fig. 9C) was preserved in a void space within the bark. However, organically associated spores were not present. Bullate globose bodies (Fig. 9D) were commonly found within tracheid lumina and were identified as putative oogonia.

4.4. Host–fungus interactions

The responses of extant infected plants to fungal invasion involve a range of physical and chemical defenses used to retard further invasion (Bennet and Wallsgrove, 1994; Sadavasian and Thayumanavan, 2003; Schwarze, 2007; Stubblefield and Taylor, 1986). These defenses provide immediate resistance to stem invasion, but they may be overcome by organisms that have become adapted to them (Franceschi et al., 2000).

Interactions between fungi and vascular plants in the fossil record are usually measured based on the existence of microscopic putative plant responses to fungal invasion, such as the occurrence of tyloses, various types of resiniferous deposits originating reaction and barrier zones, abnormal growth rings, and appositions (Stubblefield and Taylor, 1986; Weaver et al., 1997; Falcon-Lang et al., 2001; Taylor and Krings, 2005; Krings et al., 2007; Pujana et al., 2009; Harper et al., 2012; Gnaedinger et al., 2015; McLoughlin and Bomfleur, 2016; Sagasti et al., 2019).

In our material the interaction is documented by microscopic responses developed in both the bark of the infected plant and more expressively in the xylem tissue, being represented by putative reaction zones, barrier zones and wall apposition process.

The physical evidence here interpreted as host response processes to fungal attack could alternatively be linked to resins which occur in the ray cells and axial tracheids as resin plugs in the wood of extant araucarians (Stockey, 1982; Jane, 1956). Their mode of occurrence is distinguished from that of other conifers by the absence of resin canals or resin cells. However, the uncommon abundance of dark content in the branch under study and the similarity with records of both extant conifer woods (Schwarze, 2007) and fossil woods attacked by fungi (Pujana et al., 2009; Feng et al., 2015; Gnaedinger et al., 2015; Sagasti et al., 2019) point to physical evidence of plant-fungus interactions.

4.4.1. Bark

The preservation of the bark, showing diffused, extensively decayed areas (Fig. 7A) rather than precisely delimited attacked zones, made it difficult to identify mutualistic, saprophytic or parasitic relationships between fungi and the host.

However, the comparison of fungal infestation in a conifer wood from the Jurassic of Patagonia with symptoms on extant trees showed that phloem infection can promote hypersensitive responses that lead to the accumulation of resins and other defensive chemicals in the cells surrounding the attack site (Sagasti et al.,

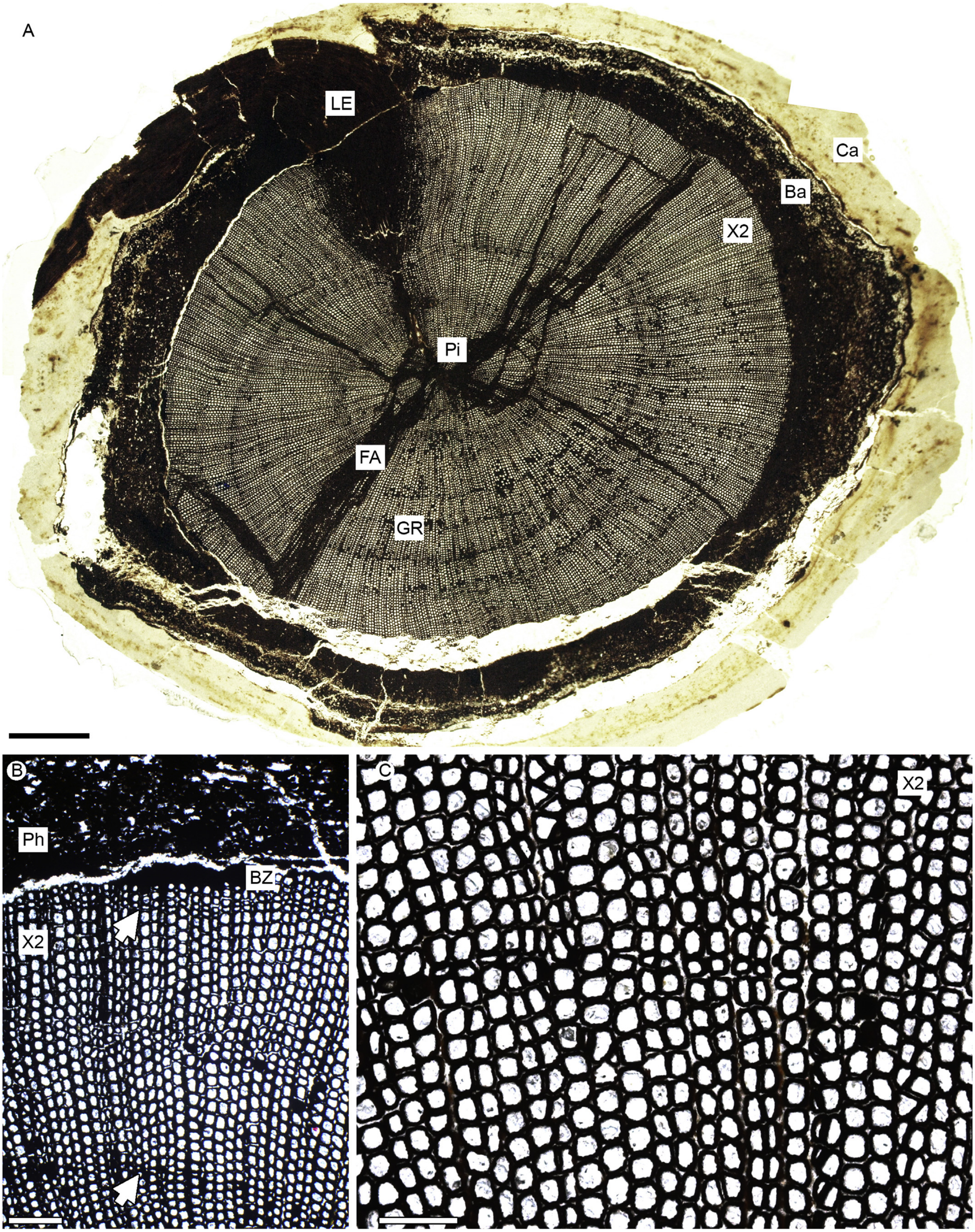

Fig. 4. Gross morphology of the secondary branch in cross-section (slide 2443-Pb-1). A) Composite image of a full cross-section under stereoscopic microscope showing the carbonate layer (Ca), irregular pith (Pi), the massive, homogeneous secondary xylem (X2), the growth rings of variable width (GR), a leaf emergence (LE), the bark (Ba) and fungal attack (FA); B) detail of the secondary xylem showing uneven growth rings (arrows); C) growth ring boundary. Scale bars: A) 2 mm; B, C) 200 μm.

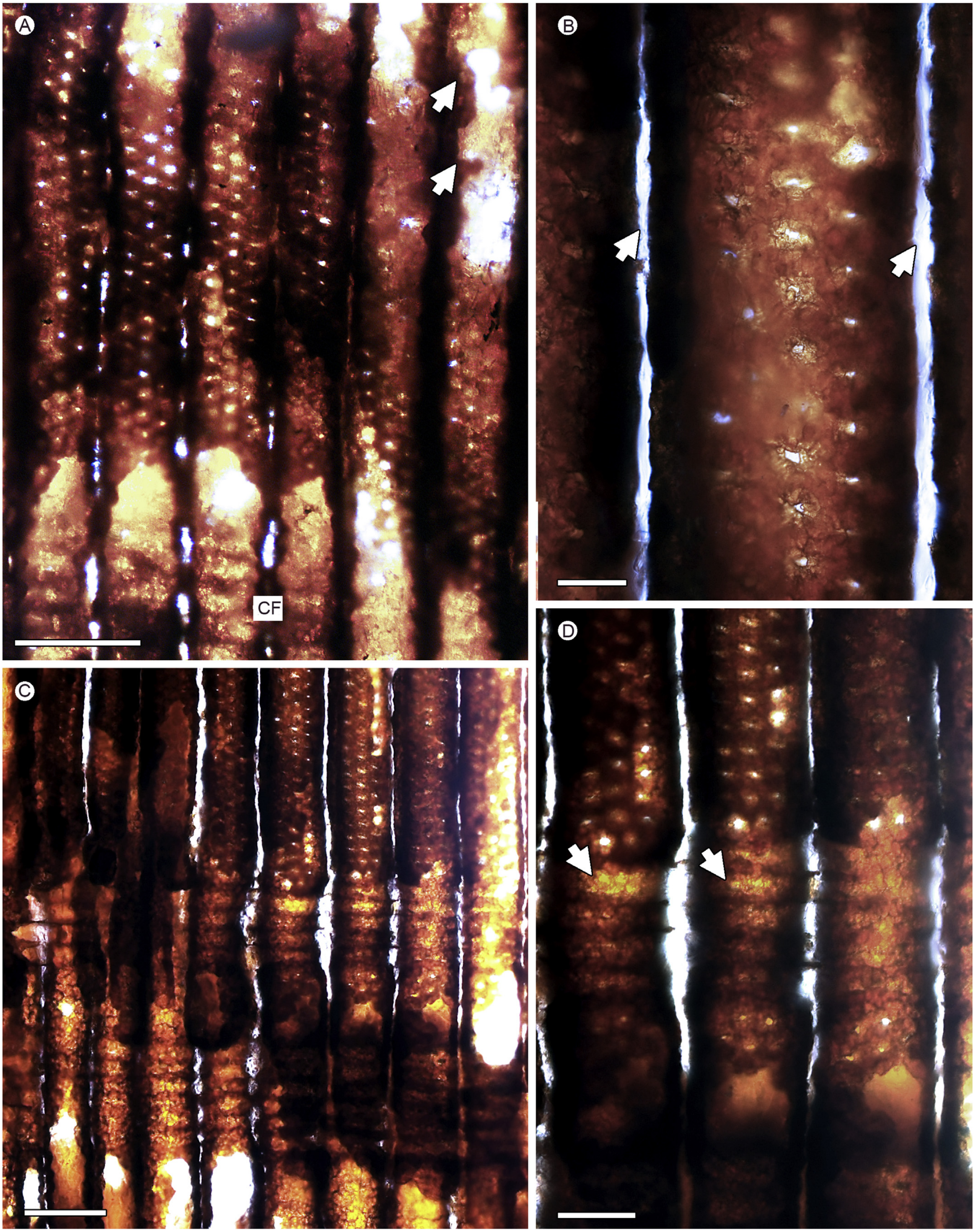

Fig. 5. Main anatomical wood pattern in radial section (slide 2443-Pb-8). A) Elongate tracheids, crossfields (CF) and evidence of fungal attack (arrows). B) detail of a tracheid showing crowded triseriate, alternate hexagonal areolated pitting in compact, margin to margin arrangement and decayed middle lamella (arrows); C) tracheids with multiseriate hexagonal areolate pitting and crossfield with araucarioid pitting; D) detail of hexagonal pitting in crossfields (arrows). Scale bars: A, C) 100 μm; B) 20 μm; D) 50 μm.

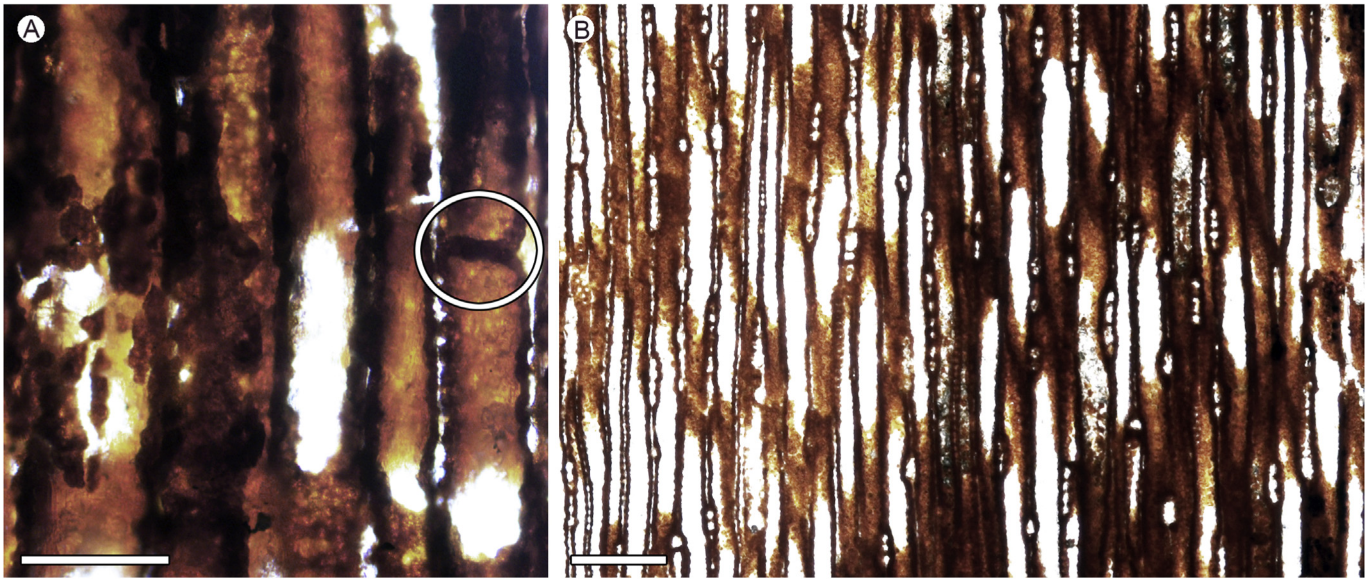

Fig. 6. Longitudinal sections. A) Resin plug inside tracheid in radial section (encircled) (slide 2443-Pb-13); B) tangential section showing uniseriate rays (slide 2443-Pb-22). Scale bars: A) 50 μm; B) 200 μm.

2019). In our material, putative reaction zones characterized by dark contents in the non-conducting collapsed phloem point to the existence of a pathogenic pattern of fungal attack (Fig. 10A, B) and indicate that the bark was probably the primary site of invasion (Fig. 10C, D).

4.4.2. Xylem

The massive, discontinuous, dark bands occurring in the peripheral secondary xylem (Fig. 11A, B) contain a dark substance deposited inside the cell lumina that completely saturates the cell walls; in extant plants, these have been attributed to barrier zones or chemical boundaries (Shain, 1967, 1971, 1979; Shigo and Marx, 1977; Shortle and Smith, 1990; Smith, 2006) and induced chemical reactions to injuries (Bauch, 1984). Evidence of these chemical barriers in fossil wood has also been found by other authors (such as Pujana et al., 2009; Gnaedinger et al., 2015).

The expressively enlarged primary and secondary wall layers found in cells at the margin of the secondary xylem (immediately next to the occurrence of barriers) suggests a host reaction relating to a wall-apposition process (Fig. 11C, D) that partially occludes the cell lumen and may have blocked hyphae growth (Aist, 1976; Shigo and Shortle, 1979). Evidence of apposition walls has previously been registered in Triassic decayed gymnosperms (Stubblefield and Taylor, 1986) and in Jurassic conifers (Feng et al., 2015; Sagasti et al., 2019). In extant plants, the occurrence of fungal bodies and hyphae inside the cell lumina (Fig. 11C, D), which shows evidence of apposition, distinguishes the chemical defenses caused by fungal degradation from those caused by wounds (Schweingruber, 2007).

In extant trees, the abundance of tracheids filled with a dark content occurring in isolation or clustered in small groups without forming a laterally continuous morphological barrier are recognized as being relicts of reaction zones (Blanchette et al., 1990; Boddy and Rayner, 1983; Pearce and Rutherford, 1981; Shain, 1967, 1971, 1979; Smith, 2006). Such anatomical evidence in decayed fossil wood may likely document host cell reactions to fungal attack (Fig. 11E, F) (Pujana et al., 2009; Feng et al., 2015).

The development of these putative defense mechanisms occurring in the secondary xylem are inferred from different chemical and anatomical evidence and through comparisons with modern analogues, and indicate that the fungal attack occurred while the host was still alive.

4.5. Degradation pattern in secondary xylem

The secondary xylem has a degradation pattern characterized by the extensive loss of middle lamella, which is composed of lignin and pectin. Tracheids (Fig. 12) are decayed in various degrees under this process. The dissolution of the lamella gradually intensifies, until the adjacent tracheids are eventually separated from each other (Fig. 12A–D). In addition, cell walls are partially decayed and are thinned by the progressive decomposition of cellulose, hemicelluloses, and lignin. However, in the intercellular system, the presence of fungal remains in voids that were previously occupied by the middle lamella (Fig. 12D) is not decisive evidence of decay from a direct fungal attack, because decay of the middle lamella in extant plants occurs through enzymatic degradation (Schwarze, 2007).

Infrequently in cross section, some tracheids show decay of the secondary wall only and other tracheids show degradation of the middle lamella (Fig. 12E). As it is difficult to establish clear boundaries between the distinct rot decay patterns of delignification that co-occur in the single secondary wood branch, we agree with Eaton (2000), who stated that rigid boundaries between different types of fungal decay are not currently appropriate.

The progressive degradation has formed small, irregular, empty pockets within the wood that are mainly observable in cross and longitudinal sections (Fig. 13A, B), sometimes surrounded by dark irregular rings probably corresponding to reaction zones (Fig. 13B). However, the most conspicuous type of degradation is that of long and continuous bands showing straight orientation and anastomosed pattern (Fig 13C–E), sometimes reaching the pith, in which the parenchymatous and sclerenchymatous tissues show no clear direct or indirect evidence of fungal attack.

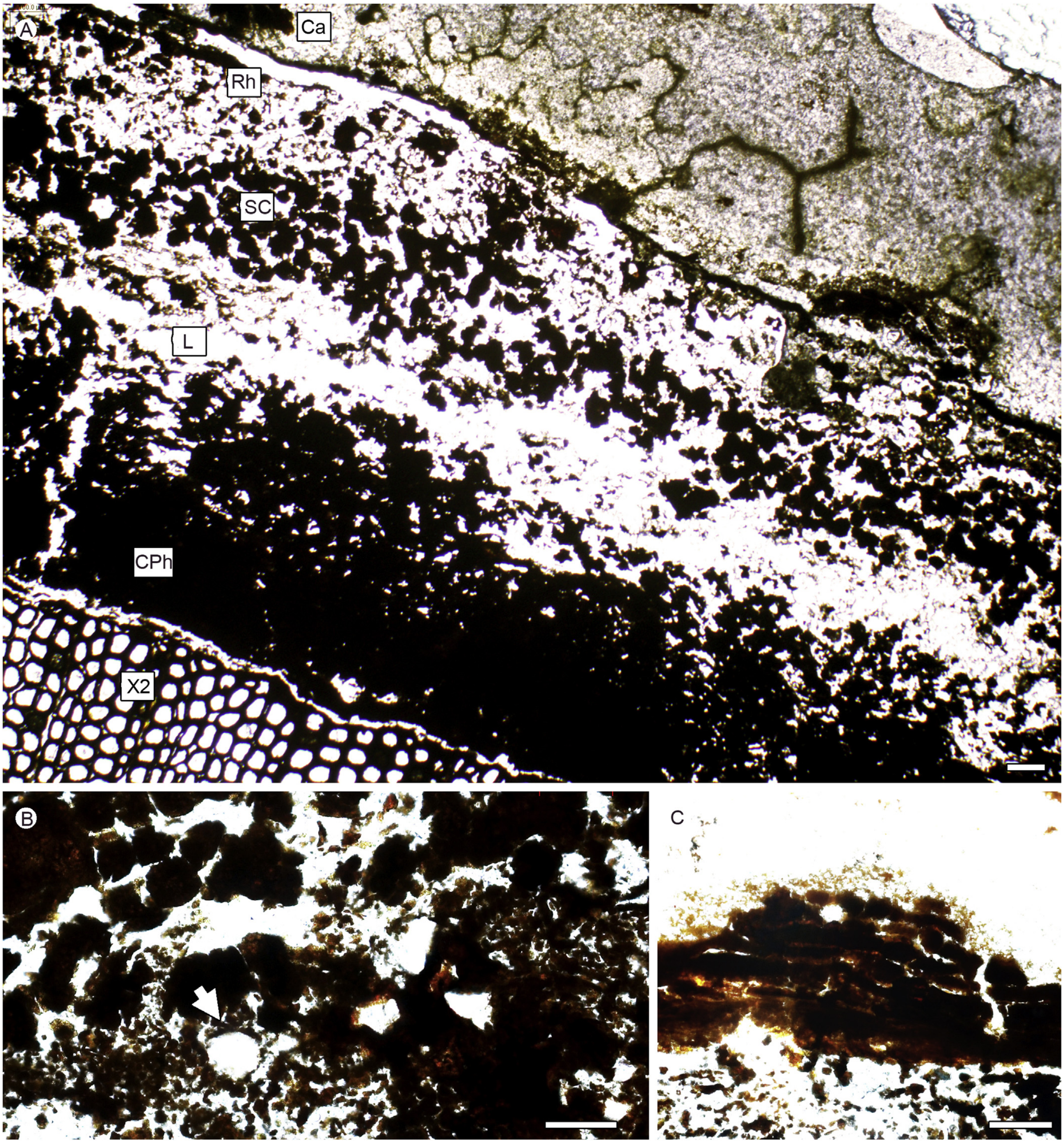

Fig. 7. Main anatomical bark pattern (slide 2443-Pb-3). A) Cross-section showing lacuna (L), belt of stone cells (SC), vestigial rhytidome (Rh) and collapsed phloem (CPh); B) canal in cross section (arrow); D) lenticel in cross section. Ca: carbonate layer. Scale bars: A, C) 100 μm; B) 50 μm.

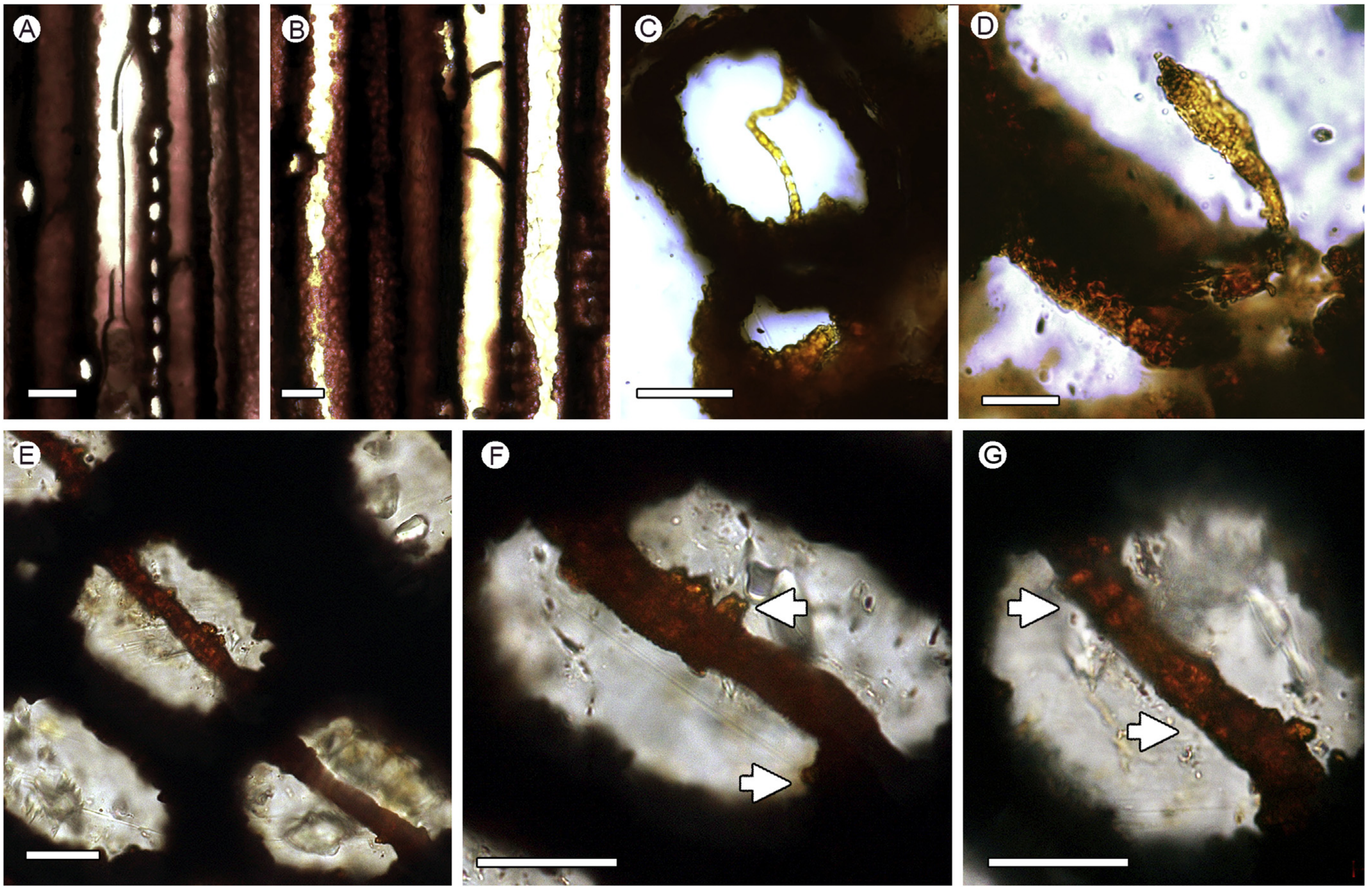

Fig. 8. Fungal hyphae in tangential (A–B) and cross-sections (C–G) of the secondary xylem. A, B) Non-septate, relatively straight smooth-walled tubular hyphae extending parallel to the tracheid axis and cross cutting tracheid walls respectively (slide 2443-Pb-26); C) regularly septate tubular hypha with curved course cross-cutting tracheid walls (slide 2443-Pb-5); D) ellipsoidal terminal hyphal swelling physically connected to a portion of the intercellular parental hypha (slide 2443-Pb-6); E) straight, unbranched tubular hyphae crossing cell walls (slide 2443-Pb-7); F) hypha with lateral, randomly arranged emergencies (arrows) (slide 2443-Pb-7); G) hypha showing transversal septa (arrows) connected to the hypha walls at right angles (slide 2443-Pb-7). Scale bars: A, B) 50 μm; C, E-G) 20 μm; D) 10 μm.

The loss of wood integrity is evident within the continuous bands, and this ultimately resulted in the breakdown and collapse of cell walls (Fig. 13D, E). Despite the dense occurrence of cell wall fragments within these bands, there is no development of damaged pockets that are devoid of cells inside the bands. However, the damage pattern points to parasitic rather than saprophytic decay, which would show a more diffuse pattern of attack (Creber and Ash, 1990).

In longitudinal section, the secondary wood also displays decayed cells with U-shaped notches or fusiform features and erosion troughs; almost all of these are restricted to the lumen of single cells (Fig. 13F) and do not coalesce into longer or wider pockets. The honeycomb-like degradation pattern occurring in extant plants, however, is the result of the coalescence of cellular degradation processes (Schwarze, 2007).

The absence of expressive damage pockets in the wood as a consequence of progressive decay validates the hypothesis that after the initial reaction from the host, decay was inhibited early by sedimentary entombment, and mineralization ensued very rapidly from the quick burial of the branch.

The microscopic features of the decayed wood in the araucarian branch investigated here correspond with those caused by extant wood rot fungi (Schmidt, 2006); they are consistent with white rot decay patterns caused by basidiomycetes and certain ascomycetes, being similar to the selective white rot decay defined by Schwarze et al. (1995) and Schwarze (2007).

The selective delignification described in our material occurs in both extant broad-leafed trees and conifers; however, the simultaneous rot, which is absent in the araucarian branch under study, occurs mainly in broad-leafed trees and seldom in conifers (Schwarze and Baum, 2000).

It has been determined that the higher lignin content of gymnosperms (composed of guaiacyl monomers) compared to angiosperms (composed of guaiacyl and syringyl monomers) is the main factor involved in the pattern of white rot, being the dominant decay type in extant angiosperm trees from the Cretaceous to the present (Ryvarden and Gilbertson, 1993; Whetten and Sederoff, 1995; Floudas et al., 2012).

A model of host evolution suggested by Krah et al. (2018) shows that brown fungi in extant floras are generalists or gymnosperm specialists, whereas most white rot fungi are angiosperm specialists. It is considered that angiosperms were a new mega niche, and white rot fungi exploited them well, which led to the high specialization rate.

The effectiveness of white rot attack on extant Araucariaceae was tested by Modes et al. (2012) by evaluating the natural resistance of the wood of different angiosperm and gymnosperm specimens after incubation with fungal colonies of Basidiomycetes, which cause white

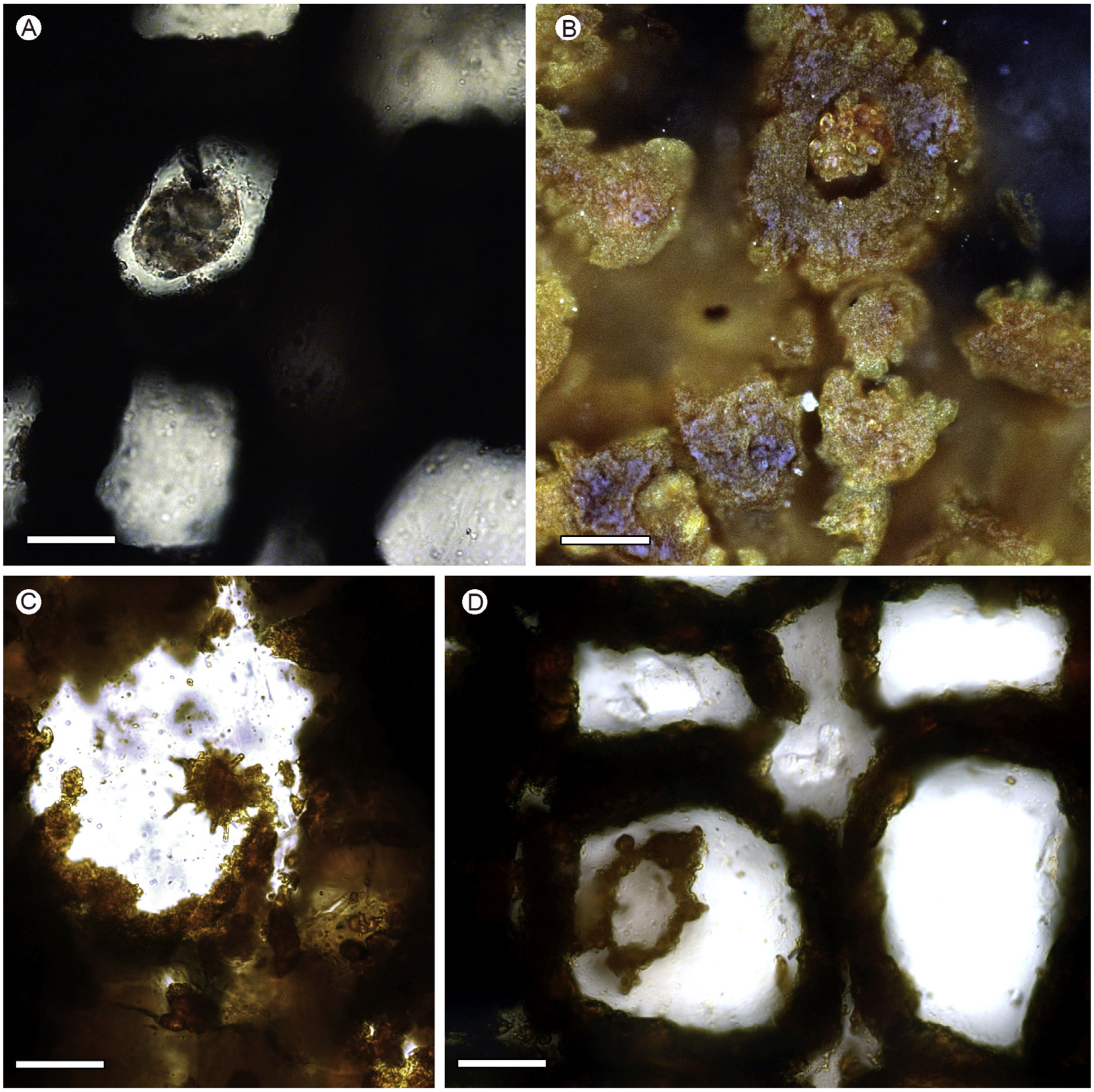

Fig. 9. Fungal bodies in the secondary xylem (A, D) and bark (B–C) in cross-sections. A, B) Arbuscule-like structures composed of several thick-walled bodies attached to the cell wall by a hypha corresponding to microsclerotia (slide 2443-Pb-2); C) putative incomplete apically branched conidiophore bearing a series of radiating short arms preserved in a void space within the bark (slide 2443-Pb-4); D) bullate globose body identified as putative fungal oogonium commonly found within tracheid lumina (slide 2443-Pb-4). Scale bars: 20 μm.

rot decay. Angiosperm forms were classified as being very resistant to resistant, whereas the gymnosperm *Araucaria angustifolia* was classified as being moderately resistant, which corresponds to the greatest loss of mass and lower mass specific apparent.

Martínez et al. (2005) indicated that the ability to degrade or modify lignin is an enzymatic process that originated in the Upper Devonian in parallel with the evolution of vascular plants, whereas Nelsen et al. (2016) concluded that genomic data are directly consistent with the evolution of lignin in the Devonian. These studies agree with the oldest known indirect evidence of the involvement of basidiomycetes in cell alteration in the progymnosperm *Callyxylon* reported by Stubblefield et al. (1985) from the Upper Devonian (USA). However, records of Basidiomycete fungal bodies associated with late Paleozoic stems are scarce, and the oldest records are those of Krings et al. (2011) for the Mississipian of France and of Dennis (1969, 1970) for the middle Pennsylvanian of North America.

Reports of wood decay by white rot documented in Table 2 are from tropical, warm, cool, and cold climatic zones from the late Devonian to the Eocene. The growing number of studies in the last decades reporting symptoms of decay by basidiomycetes during the Jurassic and Cretaceous ratify the claims of Taylor and Taylor (1997), who stated that Mesozoic greenhouse conditions favored the decay process.

The same decay symptoms identified in paleoclimates with evidence of some humid seasonality are described here in an Araucariaceae branch from a thermophilous equatorial flora (Mohr et al.,

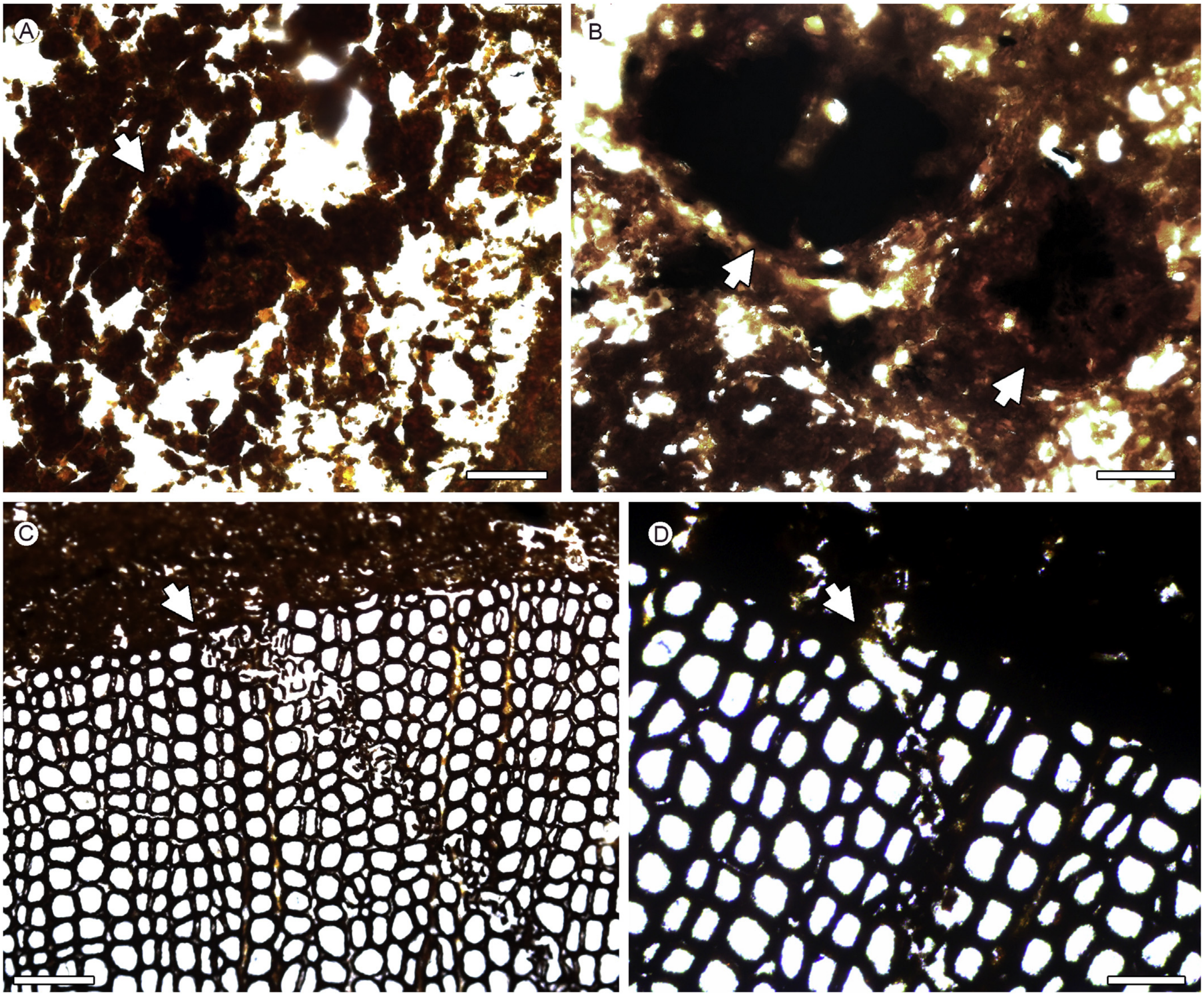

Fig. 10. Fungus-host interactions (slide 2443-Pb-1). A, B) Putative reaction zones in the bark in cross-section (arrows); C, D) putative starting decay points at the boundary of the bark with the secondary xylem (arrows). Scale bars: A) 50 µm; B, D) 100 µm; C) 200 µm.

2007) under greenhouse climate in the late Aptian within the Tropical Equatorial Hot arid belt (Chumakov et al., 1995; Hay and Floegel, 2012).

Currently, fungi are widely distributed in all terrestrial ecosystems, but relationships between latitude and diversity of possible plant pathogenic fungi indicate that climatic forces strongly drive those processes, with marked changes in diversity around middle latitudes (35°N) (Wang et al., 2019).

Extant arid ecosystems are highly sensitive to global patterns of environmental change, but models from mesic ecosystems do not apply to these environments when high temperatures and erratic moisture inputs impose a pulsed pattern on biological activities (Collins et al., 2008 and citations therein). While low moisture and high temperature certainly limit fungal activity in hot arid environments, intermittent periods of favorable temperature–moisture combination provide “windows of opportunity” that are crucial for fungal activity (Wicklow, 1981; Zak et al., 1995).

The evidence provided by the analysis of modern arid ecosystems support the inferences made here that not only was moisture important within the Aptian Tropical Equatorial Hot arid belt, but also its temporal and spatial patterning made the development of fungus–plant interactions possible. This is also in agreement with our climatic inferences based on the wood growth pattern suggesting cycles of water availability alternated with intervals of dryness in stressful growing conditions.

In addition, the presence of resting structures like microsclerotia in both bark and xylem tissues points to some exposure to adverse conditions during the period of infestation, probably as an answer to intermittent periods of dryness (Powell, 2007; Schwarze, 2007). The presence of superficial lenticels is linked to the direct exchange of oxygen, carbon dioxide, and water vapor between the internal tissues and the atmosphere; these processes occur through bark, which is otherwise impermeable (Lendzian, 2006). Some extant conifers produce lenticels in the bark of their aerial parts during summer under peak temperatures to regulate transpiration more effectively (Rosner and Kartusch, 2003).

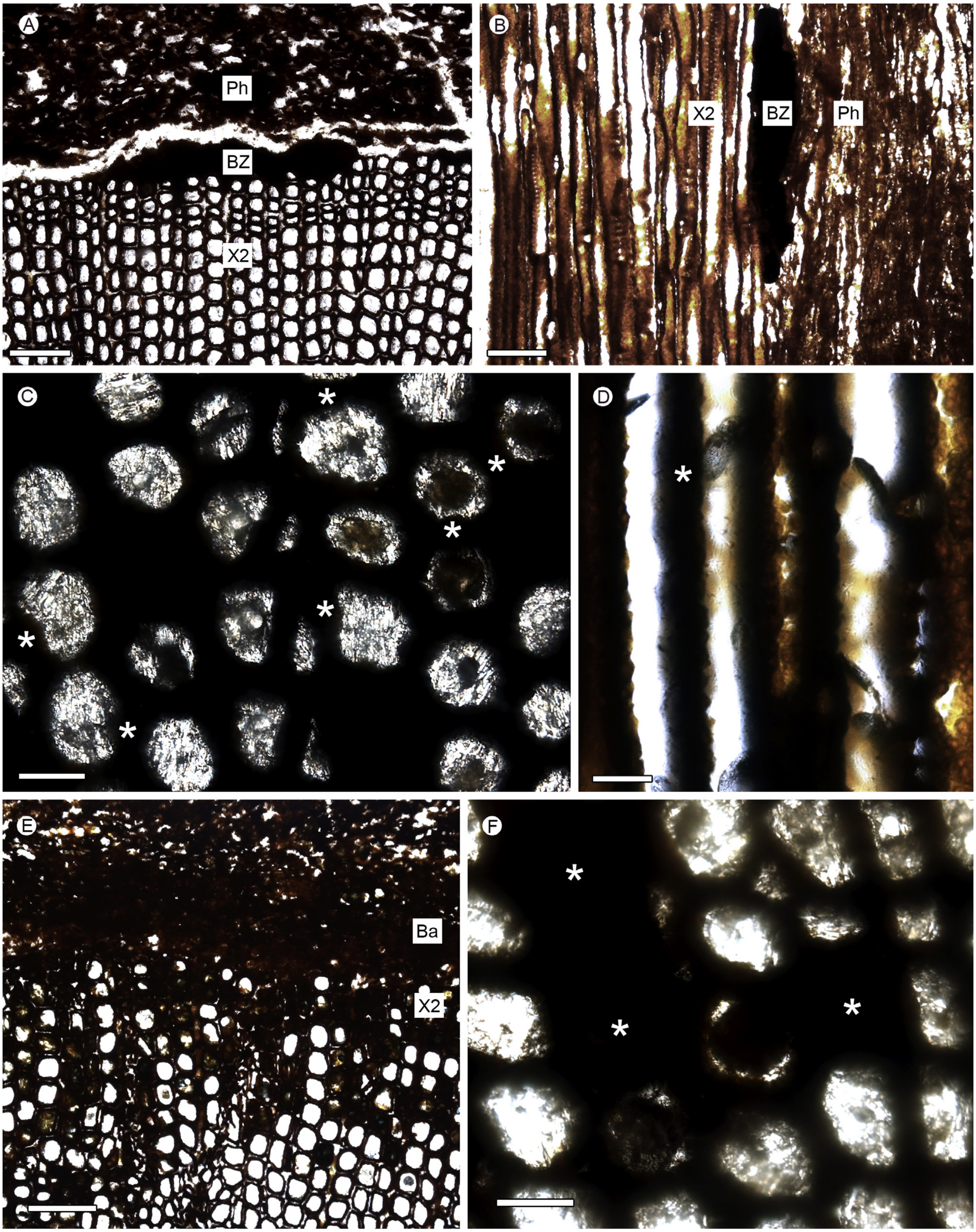

Fig. 11. Fungus-host interactions. A, B) Barrier zone at the boundary of the bark with the secondary xylem in cross (slide 2443-Pb-1) and longitudinal sections respectively (slide 2443-Pb-28); C, D) *wall-apposition process (wall thickening) and fungal bodies inside the cell lumina in cross (slide 2443-Pb-6) and longitudinal (slide 2443-Pb-30) sections; E, F) cross-sections showing *tracheids filled with dark content, isolated and in clusters (slide 2443-Pb-4); Ba: bark; BZ: barrier zone; Ph: phloem; X2: secondary xylem. Scale bars: A, B, E) 200 μm; C, D, F) 50 μm.

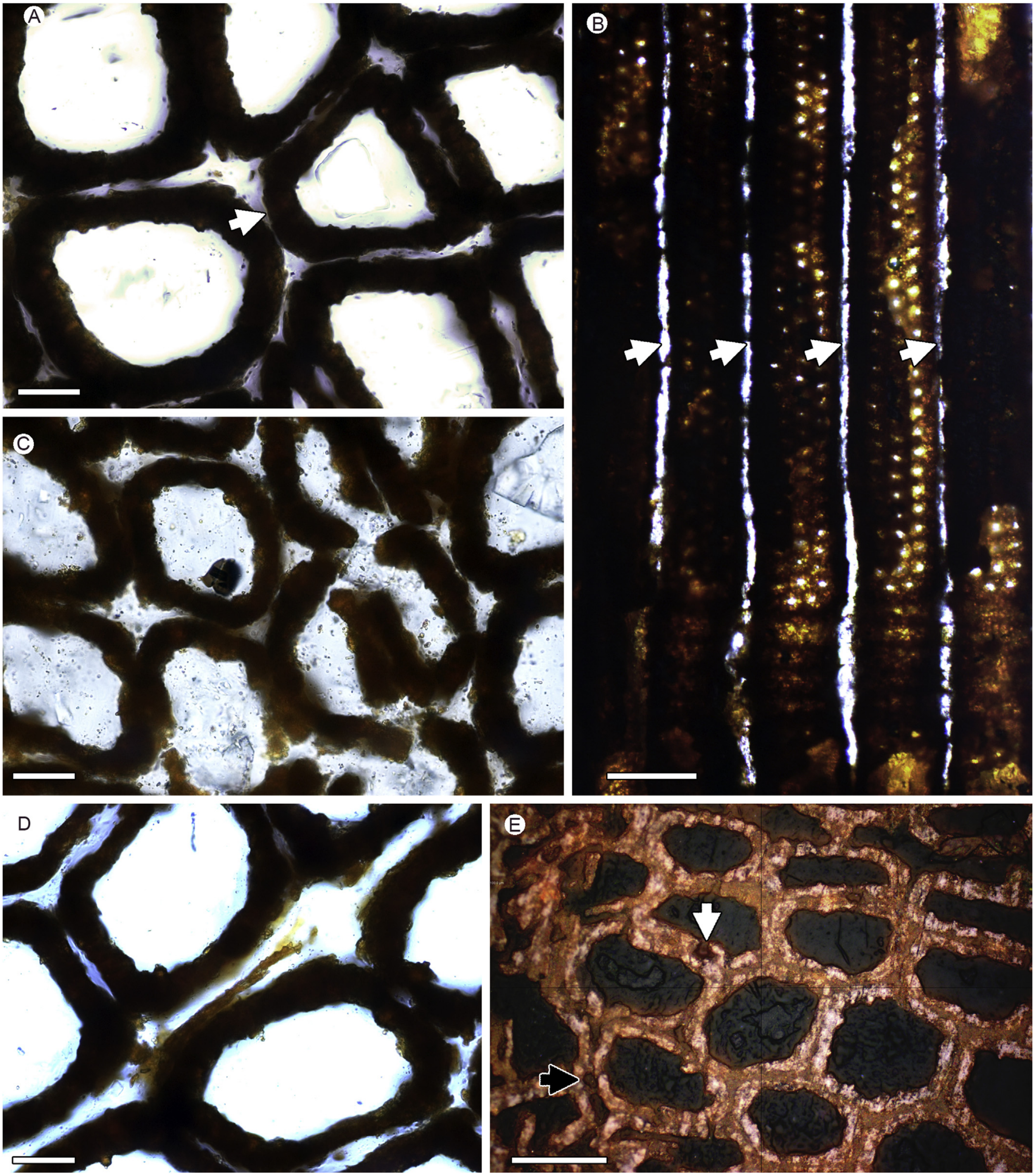

Fig. 12. Degradation of the secondary xylem. A) Cross-section showing the extensive loss of middle lamella between tracheids and cell deformation (arrow) (slide 2443-Pb-6); B) radial section showing the longitudinally continuous degradation of the middle lamella (arrows) (slide 2443-Pb-18); C) cross-section showing partially decayed cell walls (slide 2443-Pb-6); D) cells appearing as disconnected units; hypha remain in the intercellular system (slide 2443-Pb-6); E) process of decay of the secondary cell wall (white arrow) side by side with evidence of middle lamella degradation (black arrow) (slide 2443-Pb-6). Scale bars: A, C-D) 20 μm; B, E) 50 μm.

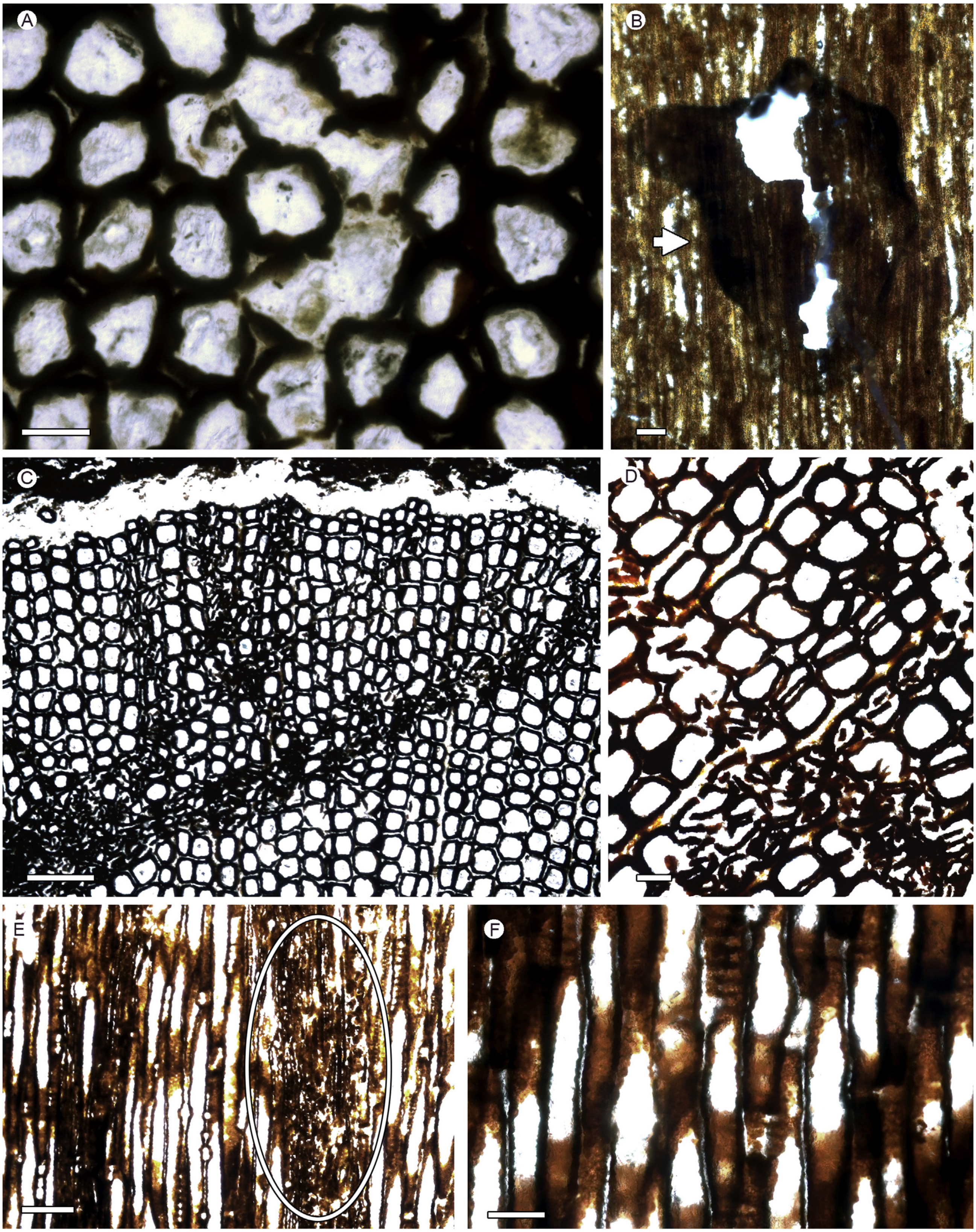

Fig. 13. Progressing degradation in the secondary xylem. A, B) small, irregular, empty pockets, in cross (slide 2443-Pb-6) and longitudinal (slide 2443-Pb-27) sections respectively, sometimes surrounded by dark irregular areas probably corresponding to reaction zones (arrow); C) elongate degraded bands, in cross-section, with straight orientation and anastomosed pattern (slide 2443-Pb-7); D, E) breakdown and collapse of the cell walls within the degraded bands in cross (slide 2443-Pb-7) and tangential (slide 2443-Pb-34) sections respectively; F) decayed cells with U-shaped notches or fusiform features and erosion troughs in longitudinal section (slide 2443-Pb-10). Scale bars: A, B, D) 50 μm; C, E) 200 μm; F) 100 μm.

5. Conclusions

This is the first study to investigate plant-fungus interactions in a complete Araucariaceae wood sample collected in the Crato Fossil Lagerstätte. Observations of three-dimensional reaction and decay patterns along the whole branch were made, and the results provide evidence of the paleoecology and climatic cycles of Aptian terrestrial ecosystems in the Tropical Equatorial Hot arid belt.

The available ecological data relating to Araucariaceae, and the growth ring patterns of the host, imply that plant growth was controlled by cyclic alternations in water availability under frequent stressing conditions. Cyclical dryness was probably related to precipitation restrictions.

The occurrence of conifers in the Crato Lagerstätte, including Araucariaceae, shows evidence that tropical humidity was high enough to support trees under greenhouse climate conditions of the early Cretaceous.

The compartmentalization process, which was detected by chemical and anatomical criteria along the phloem and mainly in the xylem tissue, indicates host-fungus interactions that are comparable with cell reactions to fungal pathogens that occur in extant living conifers, suggesting that the fungal attack begun while the plant was still alive.

The wood decay was strongly indicative of the selective pattern of white rot, which is caused by basidiomycetes and certain ascomycetes, and provided evidence that Araucariaceae had already developed defense mechanisms under the general progress of the Cretaceous greenhouse climate.

Evidence of fungus–plant interactions associated with growth ring patterns imply intermittent periods of favorable temperature-moisture inputs that were crucial for the fungal activity during the deposition interval of the Crato fossil Lagerstätte included in the Tropical Equatorial Hot arid belt.

CRediT authorship contribution statement

Ângela Cristine Scaramuzza dos Santos: Conceptualization, Data curation, Formal analysis, Writing - original draft. **Margot Guerra-Sommer:** Conceptualization, Data curation, Formal analysis, Methodology, Writing - original draft, Writing - review & editing. **Isabela Degani-Schmidt:** Data curation, Formal analysis, Writing - original draft, Writing - review & editing. **Anelise Marta Siegloch:** Data curation, Formal analysis, Writing - original draft. **Ismar de Souza Carvalho:** Funding acquisition, Project administration, Resources, Writing - original draft. **João Graciano Mendonça Filho:** Funding acquisition, Formal analysis, Resources. **Joalice de Oliveira Mendonça:** Formal analysis.

Acknowledgments

This study was conducted in association with the ongoing Research & Development project "Correlação estratigráfica, evolução paleoambiental e paleogeográfica e perspectivasexploratórias do AndarAlagoas, which is registered as ANP 180321 and sponsored by Shell Brasil under the ANP R&D levy as "Compromisso de Investimentos com pesquisa e Desenvolvimento". A.C.S.S. (141323/2017-5), M.G.S., A.M.S. (155508/2018-0), I.S.C. (303596/2016-3), J.G.M.F. acknowledge the financial support of CNPq. I.D.S. acknowledges the financial support of COPPETEC/UFRJ n° 20758. I.S.C. also acknowledges FAPERJ (E-26/202.910/2017). The authors are also grateful to Rommulo Vieira Conceição, Ana Maria Pimentel Mizusaki, and Maria Lídia Medeiros Vignol Lelarge for the insightful discussions on mineralogy and geochemistry. Two anonymous referees are also gratefully acknowledged for the assistance with improving the text.

References

Aist, J.R., 1976. Papillae and related wound plugs of plant cells. Annual Review of Phytopathology 14, 145–163.
Assine, M.L., 2007. Bacia do Araripe. Boletim de Geociencias da Petrobras 15, 371–389.
Barthel, M., Krings, M., Rößler, R., 2010. Die schwarzen Psaronien von Manebach, ihre Epiphyten, Parasiten und Pilze. Semana 25, 41–60.
Batista, M.E.P., Silva, D.C., Sales, M.A.F., Sá, A.A., Saraiva, A.A.F., Loiola, M.I.B., 2017. New data on the stem and leaf anatomy of two conifers from the Lower Cretaceous of the Araripe Basin, northeastern Brazil, and their taxonomic and paleoecological implications. PloS One 12, e0173090.
Bauch, J., 1984. Development and characteristics of discoloured wood. IAWA Journal 5, 91–98.
Bennet, R.N., Wallsgrove, R.M., 1994. Secondary metabolites in plant defence mechanisms. New Phytologist 127, 617–633.
Bernardes-de-Oliveira, M.E.C., Barreto, A.M.F., Dilcher, D., Mandarim-de-Lacerda, A.F., 2003. Isoetes eocretáceo da Formação Crato, Formação Santana, Bacia do Araripe, Nordeste do Brasil. In: Boletim de Resumos Congresso Brasileiro de Paleontologia, vol. 18. Sociedade Brasileira de Paleontologia, Brasília, p. 68.
Bernardes-de-Oliveira, M.E.C., Sucerquia, P.A., Mohr, B., Dino, R., Antonioli, L., Garcia, M.J., 2014. Indicadores paleoclimáticos na paleoflora do Crato, final do Aptiano do Gondwana Norocidental. In: Carvalho, I.S., Garcia, M.J., Lana, C.C., Strohschoen Jr., O. (Eds.), Paleontologia: Cenários de Vida – Paleoclimas, vol. 5. Interciência, Rio de Janeiro, pp. 101–119.
Blanchette, R.A., Nilsson, T., Daniel, G., Abad, A., 1990. Biological degradation of wood (Chapter 6). In: Rowell, R.M., Barbour, R.J. (Eds.), Archaeological Wood: Properties, Chemistry and Preservation. American Chemical Society, Washington, DC, pp. 141–174.
Boddy, L., Rayner, A.D.M., 1983. Deciduous in living of decay origins and content the role of moisture trees: concept of the expanded a re-appraisal decay. New Phytologist 94, 623–641.
Carvalho, I.S., 2000. Geological environments of dinosaur footprints in the intracratonic basins of northeast Brazil during the Early Cretaceous opening of the South Atlantic. Cretaceous Research 21, 255–267.
Carvalho, I.S., Agnolin, F., Aranciaga Rolando, M.A., Novas, F.E., Xavier-Neto, J., Freitas, F.I., Andrade, J.A.F.G., 2019. A new genus of pipimorph frog (anura) from the early Cretaceous Crato formation (Aptian) and the evolution of South American tongueless frogs. Journal of South American Earth Sciences 92, 222–233.
Catto, B., Jahnert, R.J., Warren, L.V., Varejão, F.G., Assine, M.L., 2016. The microbial nature of laminated limestones: lessons from the Upper Aptian, Araripe Basin, Brazil. Sedimentary Geology 341, 304–315.
Chumakov, N.M., Zharkov, M.A., Herman, A.B., Doludenko, M.P., Kalandadze, N.N., Lebedev, E.L., Ponomarenko, A.G., Rautian, A.S., 1995. Climatic belts of the mid-Cretaceous time. Stratigraphy and Geological Correlation 33, 42–63.
Coiffard, C., Mohr, B.A.R., Bernardes-de-Oliveira, M.E.C., 2013. The Early Cretaceous Aroid, *Spixiarum kipea* gen. et sp. nov., and implications on early dispersal and ecology of basal monocots. Taxon 62, 997–1008.
Coiffard, C., Mohr, B.A.R., Bernardes-De-Oliveira, M.E.C., 2014. *Hexagyne philippiana* gen. et sp. nov., a piperalean angiosperm from the Early Cretaceous of northern Gondwana (Crato Formation, Brazil). Taxon 63, 1275–1286.
Coiffard, C., Kardjilov, N., Manke, I., Bernardes-de-Oliveira, M.E.C., 2019. Fossil evidence of core monocots in the Early Cretaceous. Nature Plants 5, 691–696.
Coimbra, J.C., Arai, M., Luisa Carreño, A., 2003. Biostratigraphy of Lower Cretaceous microfossils from the Araripe basin, northeastern Brazil. Geobios 35, 687–698.
Collins, S.L., Sinsabaugh, R.L., Crenshaw, C., Green, L., Porras-Alfaro, A., Stursova, M., Zeglin, L.H., 2008. Pulse dynamics and microbial processes in aridland ecosystems. Journal of Ecology 96, 413–420.
Creber, G.T., Ash, S.R., 1990. Evidence of widespread fungal attack on Upper Triassic trees in the southwestern USA. Review of Palaeobotany and Palynology 63, 189–195.
Dennis, R.L., 1969. Fossil mycelium with clamp connections from the Middle Pennsylvanian. Science 163, 670–671.
Dennis, R.L., 1970. A Middle Pennsylvanian basidiomycete mycelium with clamp connections. Mycologia 62, 578–584.
Diéguez, C., López-Gómes, J., 2005. Fungus-plant interaction in a Thuringian (late Permian) *Dadoxylon* sp. in the SE Iberian Ranges, eastern Spain. Palaeogeography, Palaeoclimatology, Palaeoecology 229, 69–82.
Dilcher, D., Mandarim-de-Lacerda, A.F., Barreto, A.M.F., Bernardes-de-Oliveira, M.E.C., 2000. Selected fossils from the Santana Formation, Chapada do Araripe, Brazil. Revista Universidade Guarulhos Geociencias 5, 249.
Dilcher, D.L., Bernardes-de-Oliveira, M.E.C., Pons, D., Lott, T.A., 2005. Welwitschiaceae from the Lower Cretaceous of northeastern Brazil. American Journal of Botany 92, 1294–1310.
Duarte, L., 1985. Vegetais fósseis da Chapada do Araripe, Brasil. Coletânea de Trabalhos Paleontológicos. Série Geológica 27, 557–563. Paleontologia e Estratigrafia 2.
Duarte, L., 1993. Restos de araucariáceas da Formação Santana - Formação Crato (Aptiano), NE do Brasil. Anais da Academia Brasileira de Ciências 65, 357–362.
Eaton, R., 2000. A breakthrough for wood decay fungi. New Phytologist 146, 1–4.
Falcon-Lang, H.J., Cantrill, D.J., Nichols, G.J., 2001. Biodiversity and terrestrial ecology of a mid-Cretaceous, high-latitude floodplain, Alexander Island, Antarctica. Journal of the Geological Society 158, 709–724.

Fanton, J.C.M., Ricardi-Branco, F.S., Dilcher, D.L., Arruda Campos, A.C., Tavares, S.A.S., 2007a. Macrofóssil inédito de Caytoniales na Formação Crato, Cretáceo Inferior, Bacia do Araripe, NE, Brasil: Estudo preliminar. In: Carvalho, I.S., Cassab, R.C.T., Schwanke, C., Carvalho, M.A., Fernandes, A.C.S., Rodrigues, M.A.C., Carvalho, M.S.S., Arai, M., Oliveira, M.E.Q. (Eds.), Paleontologia: Cenários de Vida, vol. 1. Interciência, Rio de Janeiro, pp. 177–188.

Fanton, J.C.M., Ricardo-Branco, F., Dilcher, D., Bernardes de Oliveira, M.E.C., 2007b. *Iara iguassu*, a new taxon of aquatic angiosperm from the Crato palaeoflora (Lower Cretaceous, Santana Formation, Araripe Basin, Northeastern Brazil). UNESP Geociências 25, 211–216.

Feild, T.S., Arens, N.C., Doyle, J.A., Dawson, T.E., Donoghue, M.J., 2004. Dark and disturbed: a new image of early angiosperm ecology. Paleobiology 30, 82–107.

Feng, Z., Schneider, J.W., Labandeira, C.C., Kretzschmar, R., Rößler, R., 2015. Papillae and related wound plugs of plant cells. Annual Review of Phytopathology 14, 145–163.

Floudas, D., Binder, M., Riley, R., Barry, K., Blanchette, R.A., Henrissat, B., Martínez, A.T., Otillar, R., Spatafora, J.W., Yadav, J.S., Aerts, A., Benoit, I., Boyd, A., Carlson, A., Copeland, A., Coutinho, P.M., De Vries, R.P., Ferreira, P., Findley, K., Foster, B., Gaskell, J., Glotzer, D., Górecki, P., Heitman, J., Hesse, C., Hori, C., Igarashi, K., Jurgens, J.A., Kallen, N., Kersten, P., Kohler, A., Kües, U., Kumar, T.K.A., Kuo, A., LaButti, K., Larrondo, L.F., Lindquist, E., Ling, A., Lombard, V., Lucas, S., Lundell, T., Martin, R., McLaughlin, D.J., Morgenstern, I., Morin, E., Murat, C., Nagy, L.G., Nolan, M., Ohm, R.A., Patyshakuliyeva, A., Rokas, A., Ruiz-Dueñas, F.J., Sabat, G., Salamov, A., Samejima, M., Schmutz, J., Slot, J.C., John, F.S., Stenlid, J., Sun, H., Sun, S., Syed, K., Tsang, A., Wiebenga, A., Young, D., Pisabarro, A., Eastwood, D.C., Martin, F., Cullen, D., Grigoriev, I.V., Hibbett, D.S., 2012. The Paleozoic origin of enzymatic lignin decomposition reconstructed from 31 fungal genomes. Science 80, 1715–1719.

Franceschi, V.R., Krokene, P., Krekling, T., Christiansen, E., 2000. Phloem parenchyma cells are involved in local and distant defense responses to fungal inoculation or bark-beetle attack in Norway spruce (Pinaceae). American Journal of Botany 87, 314–326.

García-Massini, J.L., Falaschi, P., Zamuner, A.B., 2012. Fungal–arthropod–plant interactions from the Jurassic petrified forest Monumento Natural Bosques Petrificados, Patagonia, Argentina. Palaeogeography, Palaeoclimatology, Palaeoecology 329, 37–46.

Gnaedinger, S., García-Massini, J.L., Bechis, F., Zavattieri, A.M., 2015. Coniferous woods and wood-decaying fungi from the El Freno Formation (Lower Jurassic), Neuquén Basin, Mendoza Province, Argentina. Ameghiniana 52, 447–467.

Goldberg, K., Premaor, E., Bardola, T., Souza, P.A., 2019. Aptian marine ingression in the Araripe Basin: implications for paleogeographic reconstruction and evaporite accumulation. Marine and Petroleum Geology 107, 214–221.

Greguss, P., 1955. Identification of Living Gymnosperms on the Basis of Xylotomy. Akademiai Kiado, Budapest.

Insects from the Santana Formation, Lower Cretaceous of Brazil. In: Grimaldi, D.A. (Ed.), Bulletin of the American Museum of Natural History 195.

Harper, C.J., Bomfleur, B., Decombeix, A.L., Taylor, E.L., Taylor, T.N., Krings, M., 2012. Tylosis formation and fungal interactions in an early Jurassic conifer from the northern Victoria Land, Antarctica. Review of Palaeobotany and Palynology 175, 25–31.

Harper, C.J., Galtier, J., Taylor, T.N., Taylor, E.L., Rößler, R., Krings, M., 2018. Distribution of fungi in a Triassic fern stem. Earth and Environmental Science Transactions of the Royal Society of Edinburgh 108, 387–398.

Hay, W.W., Floegel, S., 2012. New thoughts about the Cretaceous climate and oceans. Earth-Science Reviews 115, 262–272.

Heimhofer, U., Hochuli, P.A., 2010. Early Cretaceous angiosperm pollen from a low-latitude succession (Araripe Basin, NE Brazil). Review of Palaeobotany and Palynology 161, 105–126.

Jane, F.W., 1956. The structure of wood, second ed. Adam and Charles Black, London.

Kerkhoff, M.L.H., Dutra, T.L., 2007. Uma Ephedraceae (Gnetales) da Bacia do Araripe, Cretáceo Inferior, Brasil. In: Carvalho, I.S., Cassab, R.C.T., Schwanke, C., Carvalho, M.A., Fernandes, A.C.S., Rodrigues, M.A.C., Carvalho, M.S.S., Arai, M., Oliveira, M.E.Q. (Eds.), Paleontologia: Cenários de Vida, vol. 1. Interciência, Rio de Janeiro, pp. 243–250.

Kershaw, P., Wagstaff, B., 2001. The southern conifer family Araucariaceae: history, status, and value for paleoenvironmental reconstruction. Annual Review of Ecology and Systematics 32, 397–414.

Krah, F.S., Bässler, C., Heibl, C., Soghigian, J., Schaefer, H., Hibbett, D.S., 2018. Evolutionary dynamics of host specialization in wood-decay fungi. BMC Evolutionary Biology 18, 119.

Krings, M., Taylor, T.N., Hass, H., Kerp, H., Dotzler, N., Hermsen, E.J., 2007. Fungal endophytes in a 400-million-year-old land plant: infection pathways, spatial distribution, and host responses. New Phytologist 174, 648–657.

Krings, M., Dotzler, N., Galtier, J., Taylor, T.N., 2011. Oldest fossil basidiomycetes clamp connections. Mycoscience 52, 18–23.

Kunzmann, L., Mohr, B.A.R., Bernardes-de-Oliveira, M.E.C., 2004. Gymnosperms from the Early Cretaceous Crato Formation (Brazil). I. Araucariaceae and *Lindleycladus* (*incertae sedis*). Fossil Record 7, 155–174.

Kunzmann, L., Mohr, B.A.R., Bernardes-de-Oliveira, M.E.C., Wilde, V., 2006. Gymnosperms from the Lower Cretaceous Crato Formation (Brazil). II. Cheirolepidiaceae. Fossil Record 9, 213–225.

Kunzmann, L., Mohr, B.A., Bernardes-de-Oliveira, M.E.C., 2007. *Novaolindia dubia* gen. et sp. nov., an enigmatic seed plant from the Early Cretaceous of northern Gondwana. Review of Palaeobotany and Palynology 147, 94–105.

Kunzmann, L., Mohr, B.A.R., Bernardes-de-Oliveira, M.E.C., 2009. *Cearania heterophylla* gen. nov. et sp. nov. a fossil gymnosperm with affinities to the Gnetales from the Early Cretaceous of northern Gondwana. Review of Palaeobotany and Palynology 158, 193–212.

Kunzmann, L., Mohr, B.A.R., Wilde, V., Bernardes-De-Oliveira, M.E.C., 2011. A putative gnetalean gymnosperm *Cariria orbiculiconiformis* gen. nov. et spec. nov. from the Early Cretaceous of northern Gondwana. Review of Palaeobotany and Palynology 165, 75–95.

Löwe, S.A., Mohr, B.A., Coiffard, C., Bernardes-de-Oliveira, M.E.C., 2013. *Friedsellowia gracilifolia* gen. nov. et sp. nov., a new gnetophyte from the Lower Cretaceous Crato Formation (Brazil). Palaeontographica Abteilung B 289, 139–177.

Lendzian, K.J., 2006. Survival strategies of plants during secondary growth: barrier properties of phellems and lenticels towards water, oxygen, and carbon dioxide. Journal of Experimental Botany 57, 2535–2546.

Lima, F.J., Saraiva, A.A.F., Silva, M.A.P., Bantim, R.A.M., Sayão, J.M., 2014. A new angiosperm from the Crato Formation (Araripe Basin, Brazil) and comments on the Early Cretaceous Monocotyledons. Anais da Academia Brasileira de Ciências 86, 1657–1672.

Martínez, A.T., Speranza, M., Ruiz-Dueñas, F.J., Ferreira, P., Camarero, S., Guillén, F., Martínez, M.J., Gutiérrez, A., Del Río, J.C., 2005. Biodegradation of lignocellulosics: microbial, chemical, and enzymatic aspects of the fungal attack of lignin. International Microbiology 8, 195–204.

Martill, D.M., Bechly, G., 2007. Introduction to the Crato Formation. In: Martill, D.M., Bechly, G., Loveridge, R.F. (Eds.), The Crato Fossil Beds of Brazil – Window into an Ancient World. University Press, Cambridge, pp. 3–7.

Matos, R.M.D., 1992. The Northeast Brazilian Rift System. Tectonics 11, 766–791.

McLoughlin, S., Bomfleur, B., 2016. Biotic interactions in an exceptionally well preserved osmundaceous fern rhizome from the Early Jurassic of Sweden. Palaeogeography, Palaeoclimatology, Palaeoecology 464, 86–96.

Modes, K.S., Lazarotto, M., Beltrame, R., Vivian, M.A., Santini, E.J., Fátima, M., Muniz, B., 2012. Resistência natural das madeiras de sete espécies florestais ao Fungo *Pycnoporus sanguineus* Causador da podridão-branca. Cerne 18, 407–411.

Mohr, B.A.R., Bernardes de Oliveira, M.E.C., 2004. *Endressinia brasiliana*, a magnolialean angiosperm from the Lower Cretaceous Crato Formation (Brazil). International Journal of Plant Sciences 165, 1121–1133.

Mohr, B.A.R., Eklund, H., 2003. *Araripia florifera* nov. gen. et sp. a putative lauralean angiosperm from the Lower Cretaceous Crato Formation (Brazil). Review of Palaeobotany and Palynology 126, 279–292.

Mohr, B.A.R., Rydin, C., 2002. *Trifurcatia flabellata* n. gen. et n. sp., a putative monocotyledon angiosperm from the Lower Cretaceous Crato Formation (Brazil). Mitteilung aus dem Museum für Naturkunde Berlin. Geowissenschaftliche Reihe 5, 335–344.

Mohr, B.A.R., Bernardes-de-Oliveira, M.E.C., Barale, G., Ouaja, M., 2006. Palaeogeographic distribution and ecology of *Klitzschophyllites*, an early Cretaceous angiosperm in southern Laurasia and northern Gondwana. Cretaceous Research 27, 464–472.

Mohr, B.A.R., Bernardes-de-Oliveira, M.E.C., Loveridge, R.F., 2007. The macrophyte flora of the Crato Formation. In: Martill, D.M., Bechly, G., Loveridge, R.F. (Eds.), The Crato Fossil Beds of Brazil – Window into an Ancient World. University Press, Cambridge, pp. 537–565.

Mohr, B.A.R., Bernardes-de-Oliveira, M.E.C., Taylor, D.W., 2008. *Pluricarpellatia*, a nymphaealean angiosperm from the Lower Cretaceous of northern Gondwana (Crato Formation, Brazil). Taxon 57, 1147–1158.

Mohr, B.A.R., Schultka, S., Suess, H., Bernardesde-Oliveira, M.E.C., 2012. A new drought resistant gymnosperm taxon *Duartenia araripensis* n. gen. et sp. (Cheirolepidiaceae?) from the Early Cretaceous of Northern Gondwana. Palaeontographica Abteilung B 289, 1–25.

Mohr, B.A.R., Coiffard, C., Bernardes-de-Oliveira, M.E.C., 2013. *Schenkeriphyllum glanduliferum*, a new magnolialean angiosperm from the Early Cretaceous of Northern Gondwana and its relationship to fossil and modern Magnoliales. Review of Palaeobotany and Palynology 189, 57–72.

Mohr, B.A.R., Bernardes de Oliveira, M.E.C., Loveridge, R., Pons, D., Sucerquia, P.A., Castro-Fernandes, M.C., 2015. *Ruffordia goeppertii* (Schizaeales, Anemiaceae) a common fern from the Lower Cretaceous Crato Formation of northeast Brazil. Cretaceous Research 54, 17–26.

Naish, D., 2007. Turtles of the Crato Formation. In: Martill, D.M., Bechly, G., Loveridge, R.F. (Eds.), The Crato Fossil Beds of Brazil – window into an Ancient World. University Press, Cambridge, pp. 452–457.

Nelsen, M.P., DiMichele, W.A., Peters, S.E., Boyce, C.K., 2016. Delayed fungal evolution did not cause the Paleozoic peak in coal production. Proceedings of the National Academy of Sciences 113, 2442–2447.

Neumann, V.H., Borrego, A.G., Cabrera, L., Dino, R., 2003. Organic matter composition and distribution through the Aptian-Albian lacustrine sequences of the Araripe Basin, northeastern Brazil. International Journal of Coal Geology 54, 21–40.

Pearce, R.B., Rutherford, J., 1981. A wound-associated suberized barrier to the spread of decay in the sapwood of oak (*Quercus robur* L.). Physiological Plant Pathology 19, 359–369.

Philippe, M., Bamford, M.K., 2008. A key to morphogenera used for Mesozoic conifer-like woods. Review of Palaeobotany and Palynology 148, 184–207.

Pinheiro, F.L., Horn, B.L.D., Schultz, C.L., De Andrade, J.A.F.G., Sucerquia, P.A., 2012. Fossilized bacteria in a Cretaceous pterosaur headcrest. Lethaia 45, 495–499.

Ponte, F.C., Appi, C.J., 1990. Proposta de revisão da coluna litoestratigráfica da Bacia do Araripe. In: Anais Congresso Brasileiro de Geologia, vol. 36. Sociedade Brasileira de Geologia, Natal, pp. 211–226.

Powell, M.R., 2007. A model for probabilistic assessment of phytosanitary risk reduction measures. Plant Disease 86, 552–557.
Pujana, R.R., García-Massini, J.L., Brizuela, R.R., Burrieza, H.P., 2009. Evidence of fungal activity in silified gymnosperm wood from the Eocene of southern Patagonia (Argentina). Geobios 42, 639–647.
Ricardi-Branco, F., Torres, M., Tavares, S.S., de Souza, I.S., Tavares, P.G., Campos, A.C.A., 2013. *Itajuba yansanae* gen. and sp. nov. of Gnetales, Araripe Basin (Albian-Aptian) in Northeast Brazil (Chapter 7). In: Ray, P., Zhang, Y. (Eds.), Climate Change and Regional/Local Responses. InTech, Zagreb, pp. 187–205.
Richter, H.G., Grosser, D., Heinz, I., Gasson, P.E., 2004. IAWA list of microscopic features for softwood identification. IAWA Journal 25, 1–70.
Rios-Netto, A.M., Regali, M.S.P., Carvalho, I.S., Freitas, F.I., 2012. Palinoestratigrafia do intervalo Alagoas da Bacia do Araripe, Nordeste do Brasil. Revista Brasileira de Geociencias 42, 331–342.
Rosner, S., Kartusch, B., 2003. Structural changes in primary lenticels of Norway spruce over the seasons. IAWA Journal 24, 105–116.
Rydin, C., Mohr, B.A.R., Friis, E.M., 2003. *Cratonia cotyledon* gen. et sp. nov. A unique Cretaceous seedling related to *Welwitschia*. Proceedings of the Royal Society London, Series B 270, 29–32.
Ryvarden, L., Gilbertson, R.L., 1993. European polypores Part 1: *Abortiporus – Lindtneria*. Fungiflora, Oslo.
Sadasivan, A.J., Thayumanayan, B., 2003. Molecular Host Plant Resistance to Pests. Marcel Dekker, New York.
Sagasti, A.J., García-Massini, J.L., Escapa, I.H., Guido, D.M., 2019. Multitrophic interactions in a geothermal setting: arthropod borings, actinomycetes, fungi and fungal-like microorganisms in a decomposing conifer wood from the Jurassic of Patagonia. Palaeogeography, Palaeoclimatology, Palaeoecology 514, 31–44.
Scherer, C.M.S., Goldberg, K., Bardola, T., 2015. Facies architecture and sequence stratigraphy of an early post-rift fluvial succession, Aptian Barbalha Formation, Araripe Basin, northeastern Brazil. Sedimentary Geology 322, 43–62.
Schmidt, O., 2006. Wood and Tree Fungi. Springer, Berlin.
Schwarze, F.W.M.R., 2007. Wood decay under the microscope. Fungal Biology Reviews 21, 133–170.
Schwarze, F.W.M.R., Baum, S., 2000. Mechanisms of reaction zone penetration by decay fungi in wood beech (*Fagus sylvatica*). New Phytologist 146, 129–140.
Schwarze, F.W.M.R., Lonsdale, D., Fink, S., 1995. Soft rot and multiple T-branching by the basidiomycete *Inonotus hispidus* in ash and London plane. Mycological Research 99, 813–820.
Schweingruber, F.H., 1996. Tree Rings and Environment - Dendroecology. Haupt Press, Berne.
Schweingruber, F.H., 2007. Wood Structure and Environment. Springer, Berlin.
Scotese, C.R., 2011. Paleogeographic and Paleoclimatic atlas. AAPG Search and Discovery Article #30193. http://www.searchanddiscovery.com/pdfz/documents/2011/30193scotese/ndx_scotese.pdf.html.
Scotese, C.R., 2014. Atlas of Early Cretaceous Paleogeographic Maps, PALEOMAP Atlas for ArcGIS, volume 2, The Cretaceous, Maps 23 - 31, Mollweide Projection. PALEOMAP Project, Evanston, IL. https://doi.org/10.13140/2.1.4099.4560.
Shain, L., 1967. Resistance of sapwood in stems of loblolly pine to infection by *Fomes annosus*. Phytopathology 57, 1034–1045.
Shain, L., 1971. The response of sapwood of Norway spruce to infection by *Fomes annosus*. Phytopathology 61, 301–307.
Shain, L., 1979. Dynamic responses of differentiated sapwood to injury and infection. Phytopathology 69, 1134–1137.
Shigo, A.L., Marx, H.G., 1977. Compartmentalization of decay in trees, vol. 405. USDA Forest Service Agriculture Information Bulletin, Washington, D.C.
Shigo, A.L., Shortle, W.C., 1979. Compartmentalization of discolored wood in heartwood of red oak. Phytopathology 69, 710–711.
Shortle, W.C., Smith, K.T., 1990. Decay column boundary layer formation in maple. Biodeterioration Research 3, 377–389.
Smith, K.T., 2006. Compartmentalization today. Arboricultural Journal 29, 173–184.
Souza-Lima, W., Silva, R.O., 2018. Aptian–Albian paleophytogeography and paleoclimatology from Northeastern Brazil sedimentary basins. Review of Palaeobotany and Palynology 258, 163–189.
Spicer, B., Skelton, P.W., 2003. The operation of the major geological carbon sinks (Chapter 8). In: Skelton, P.W., Spicer, R.A., Kelley, S., Gilmour, I. (Eds.), The Cretaceous World. University Press, Cambridge, pp. 249–271.
Stockey, R.A., 1982. The Araucariaceae: an evolutionary perspective. Review of Palaeobotany and Palynology 37, 133–154.
Stubblefield, S.P., Taylor, T.N., 1986. Wood decay in silicified gymnosperms from Antarctica. Botanical Gazette 147, 116–127.
Stubblefield, S.P., Taylor, T.N., Beck, C.B., 1985. Studies of Paleozoic Fungi. IV. Wood-Decaying Fungi in *Callixylon newberryi* from the Upper Devonian. American Journal of Botany 72, 1765–1774.
Sucerquia, P.A., 2006. Gimnospermas eocretáceas da Formação Crato, Bacia do Araripe, Nordeste do Brasil (Unpubl. MSc Dissertation). University of São Paulo, p. 108.
Sucerquia, P.A., Bernardes-de-Oliveira, M.E.C., Mohr, B.A.R., 2015. Phytogeographic, stratigraphic, and paleoclimatic significance of *Pseudofrenelopsis capillata* sp. nov. from the Lower Cretaceous Crato Formation, Brazil. Review of Palaeobotany and Palynology 222, 116–128.
Taylor, T.N., Krings, M., 2005. Fossil microorganisms and land plants: associations and interactions. Symbiosis 40, 119–135.
Taylor, T.N., Taylor, E.L., 1997. The distribution and interactions of some Paleozoic fungi. Review of Palaeobotany and Palynology 95, 83–94.
Tian, N., Wang, Y., Zheng, S., Zhu, Z., 2020. White-rotting fungus with clamp-connections in a coniferous wood from the Lower Cretaceous of Heilongjiang Province, NE China. Cretaceous Research 105, 104014.
Vera, E.I., Césari, S.N., 2012. Fossil wood (Coniferales) from the Baqueró Group (Aptian), Santa Cruz Province, Argentina. Anais da Academia Brasileira de Ciências 84, 617–625.
Wan, M., Yang, W., Liu, L., Wang, J., 2016. Plant-arthropod and plant-fungus interactions in late Permian gymnospermous woods from the Bogda Mountains, Xinjiang, northwestern, China. Review of Palaeobotany and Palynology 235, 120–128.
Wan, M., Yang, W., He, X., Liu, L., Wang, J., 2017. First record of fossil basiciomycete clamp connections in cordaitalean stems from the Asselian-Sakmarian (Lower Permian) of Shanxi Province, North China. Palaeogeography, Palaeoclimatology, Palaeoecology 466, 353–360.
Wang, P., Chen, Y., Sun, Y., Tan, S., Zhang, S., Wang, Z., Zhou, J., Zhang, G., Shu, W., Luo, C., Kuang, J., 2019. Distinct biogeography of different fungal guilds and their associations with plant species richness in forest ecosystems. Frontiers in Ecology and Evolution 7, 216.
Weaver, L., McLoughlin, S., Drinnan, A., 1997. Fossil woods from the Upper Permian Bainmedart Coal Measures, northern Prince Charles Mountains, East Antarctica. AGSO Journal of Australian Geology and Geophysics 16, 655–676.
Wei, X., Zhang, X., Shi, G.R., Zhao, X., Huang, X., Luan, T., 2016. First report of a phytogeographically mixed (transitional) Middle-Late Permian fossil wood assemblage from the Hami area, northwest China, and implications for Permian phytogeographical, paleogeographical and paleoclimatic evolution in central Asia. Palaeogeography, Palaeoclimatology, Palaeoecology 448, 125–140.
Wei, H.B., Gou, X.D., Yang, J.Y., Feng, Z., 2019. Fungi-plant-arthropods interactions in a new conifer wood from the uppermost Permian of China reveal complex ecological relationships and tropics networks. Review of Palaeobotany and Palynology 271, 1–14.
Whetten, R., Sederoff, R., 1995. Lignin Biosynthesis. The Plant Cell 7, 1001–1013.
Wicklow, D.T., 1981. Biogeography and conidial fungi. In: Cole, G.T., Kendrick, B. (Eds.), Biology of conidial fungi, vol. 1. Academic Press, New York, pp. 417–447.
Zak, J.C., Sinsabaugh, R., MacKay, W.P., 1995. Windows of opportunity in desert ecosystems: their implications to fungal community development. Canadian Journal of Botany 73 (S1), 1407–1414.
Ziegler, A.M., Eshel, G., McAllister Rees, P., Rothfus, T.A., Rowley, D.B., Sunderlin, D., 2003. Tracing the tropics across land and sea: Permian to present. Lethaia 36, 227–254.

Appendix A. Supplementary data

Supplementary data to this article can be found online at https://doi.org/10.1016/j.cretres.2020.104525.